III RHEOLOGY

III.1 Introductory Definitions

In the course of fiber formation from fluids such as polymer melts or polymer solutions, it is necessary to push the fluids through openings, holes, or capillaries under pressure, as well as to extend, to draw the fluids under tensional forces. Therefore, we must pay attention to the behavior of polymeric fluids under such conditions. It is necessary to know how the polymeric fluids behave when subjected to various strains and stresses.[1,2] Rheology is a very large field, so in this little introduction the subject is abbreviated "to bare bones" only. The description is limited to the theory of viscoelasticity, particularly as presented by N. W. Tschoegl[1] and A. J. Staverman and F. Schwartzl.[64] Other important aspects are treated in a sketchy way, with the exception of the slightly more detailed description of capillary flow.

If we have a cylindrical rod, and if we stretch the rod by pulling by its two ends, we supply the force, F, in the direction of the material axis. The applied force causes a deformation, elongation or extension, ΔL, of the initial length, L_0. If the extension is not excessive the deformation will be proportional to the applied force by some proportionality constant: $F = k\Delta L$, where $\Delta L = L - L_0$. If we relate the force to the cross sectional area of the specimen and the increase of length to the initial length, we obtain stress, σ, and strain, ε.

$$\sigma = E \cdot \varepsilon \tag{III.1}$$

Equation III.1 represents the formulation of the Hooke's law, where E represents the proportionality constant, known as the *modulus of elasticity.*

Another deformation type of concern is shearing, or laminar shear flow. Let us assume that we have two surfaces, A, and, B separated by the distance, Y. The space between the two surfaces is filled with a fluid, as in Figure III.1. If the bottom surface, B, is moving in relation to the surface A in the direction x, then the fluid contained between the surfaces will be subjected to a shearing force. The fluid velocity at any distance between the plates will be $v(Y)$, while the fluid velocity at each of the surfaces will remain zero. The force needed to move the surfaces, in analogy to Hooke's law, depends on the surface area and on the gradient of velocity dv/dY. The proportionality constant, η, is called *viscosity.*

$$\tau = \eta\dot{\gamma} \tag{III.2}$$

Here we designate *shearing stress*, $\tau = F/a$, and *rate of shearing*, $\dot{\gamma} = dv/dY$

Both equations, III.1 and III.2, are *constitutive equations*, equations that depend only on the nature of the material and are independent of the geometry of the body. The form of these equations was introduced by Isaac Newton, and materials which obey equation III.2 are often referred to as *Newtonian fluids.*

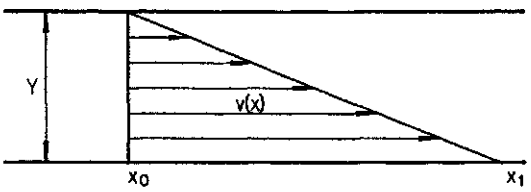

Figure III.1: *Shear flow of a fluid between surfaces.*

In the case of a cylindrical surface, like the interior of a capillary, shear stress at the wall surface, τ_w, may be calculated as

$$\tau_w = Pr/(2l) \tag{III.3}$$

where P stands for the pressure drop in the capillary of length l and of radius r. In reality, certain velocity gradients develop at the entry to the capillary, and these gradients cause some pressure losses. These losses, named after their discoverer, Couette, depend on the radius of the capillary, so equation III.3 is often given in the form which corrects for those losses:

$$\tau_w = Pr/[2(l + nr)] \tag{III.4}$$

The value of n must be determined experimentally.

The rate of shear for the flow in a capillary may be calculated as

$$\dot{\gamma} = \frac{4Q}{\pi r^3} \tag{III.5}$$

where Q is the volume of polymer flowing through the capillary in a unit of time, usually in a second.

Equation III.1 relates to materials which are purely elastic, and equation III.2 describes behavior of materials which are purely viscous. Real materials that are purely elastic or purely viscous are extremely rare; combinations of both behaviors are most common. We shall look into some of the reasons for this.

Usually, when a material is under the action of forces, the forces do not act only in one direction. Hence, it is important to examine the forces active in a body under stress. If we imagine a body in space, the forces and moments acting on this body may be characterized by resultant force elements, moment element, and a unitary vector normal to the surface being acted upon. In a Cartesian coordinate system, the state of stress in a body may be characterized by nine components resulting from three coordinates, one on each plane, and three vectors for each plane (Figure III.2). The state of stress may be represented by a second order *stress tensor*:

$$|\sigma_{ij}| = \begin{vmatrix} \sigma_{11} & \sigma_{12} & \sigma_{13} \\ \sigma_{21} & \sigma_{22} & \sigma_{23} \\ \sigma_{31} & \sigma_{32} & \sigma_{33} \end{vmatrix} \tag{III.6}$$

The components which are perpendicular to the coordinate planes are called *normal stresses* , and are on the diagonal of the tensor $(\sigma_{11}, \sigma_{22}, \sigma_{33})$. The components with "mixed" indices are called *shear stresses*. Analogously, one may derive

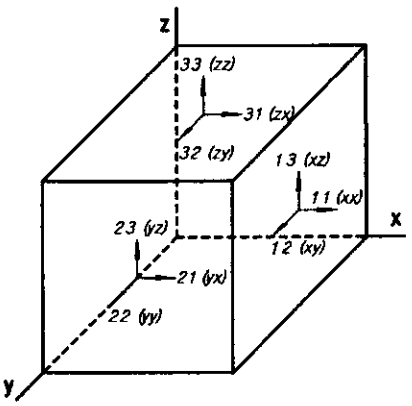

Figure III.2: *Components of the stress tensor.*

a *strain tensor* where

$$\gamma_{ij} = \frac{\frac{\partial u_i}{\partial_j} + \frac{\partial u_j}{\partial x_i}}{2} \tag{III.7}$$

$$|\gamma_{ij}| = \begin{vmatrix} \gamma_{11} & \gamma_{12} & \gamma_{13} \\ \gamma_{21} & \gamma_{22} & \gamma_{23} \\ \gamma_{31} & \gamma_{32} & \gamma_{33} \end{vmatrix} \tag{III.8}$$

Here too, the components on the diagonal are called *normal strains* and the components with "mixed" indices are called *shearing strains.*

According to the definition of deformation in simple shear $\varepsilon_{12} = \partial u_1/\partial u_2$ the corresponding strain component in simple shear is $\gamma_{12} = \partial u_1/2\partial u_2$. Thus ε_{12} may be named the *amount of shear* and γ will be the *shear strain.* In analogy to this the shear rate is twice the corresponding tensor component.

Equation III.2 may be given in terms of the tensor components:

$$\tau = G\gamma \tag{III.9}$$

where G is the *shear modulus*, $\tau = \sigma_{12}$ and $\gamma = 2\lambda_{12}$.

If a material is subjected to isotropic forces (pressure), then in agreement with equation III.7 we have:

$$p = -K(\gamma_{11} + \gamma_{22} + \gamma_{33}) \tag{III.10}$$

where K is the *bulk modulus*

Lateral contraction of a body subjected to uniaxial extension may be expressed as

$$-\gamma_{22}/\gamma_{11} = \mu \tag{III.11}$$

Here μ represents *Poisson's ratio.*

Different moduli and Poisson's ratio may be expressed by each other in a number of different ways:

$$E = \frac{9KG}{3K + G} = 3K(1 - 2) = 2G(1+) \tag{III.12}$$

$$G = \frac{3KE}{9K - E} = \frac{E}{2(1+\mu)} = \frac{3K(1-2\mu)}{2(1+\mu)} \tag{III.13}$$

$$K = \frac{GE}{9G - 3E} = \frac{2G(1+\mu)}{3(1-2\mu)} = \frac{E}{3(1-2\mu)} \tag{III.14}$$

$$\mu = \frac{E}{2G} - 1 = 0.5 - \frac{E}{6K} = \frac{3K - 2G}{6K + 2G} \tag{III.15}$$

Behavior of an elastic material may be expressed also through the *elastic compliance*:

$$\gamma = J\tau \tag{III.16}$$

where J is the *shear compliance*, and $J = 1/G$. In further analogy we have

$$\varepsilon = D\sigma \tag{III.17}$$

Here D is the *tensile compliance* or *stretch*, $D = 1/E$. Bulk modulus, K has corresponding *bulk compliance*, $B = 1/K$. Likewise one may quote the mutual interrelationships:

$$J = 2\ D\ (1+\mu) = \frac{3\,D - B}{3} = \frac{2\ B(1+\mu)}{3\,(1-2\mu)} \tag{III.18}$$

$$D = \frac{J}{2\,(1+\mu)} = \frac{B}{3\,(1-2\,\mu)} = \frac{B}{9} + \frac{J}{3} \tag{III.19}$$

$$B = 9\,D - 3\ J = \frac{3\ J\,(1-2\ \mu)}{2\,(1+\mu)} = 3\ D(1-2\ \mu) \tag{III.20}$$

$$\mu = \frac{J}{2\ D} - 1 = 0.5 - \frac{B}{6\ D} = \frac{3\ J\ 2\ B}{6\ J + 2\ B} \tag{III.21}$$

For purely linear viscous flow, in conjunction with equation III.2 we have:

$$\tau = \sigma_{12} \qquad \text{and} \qquad \dot{\gamma} = \dot{\lambda}/2 \tag{III.22}$$

The viscous analog of *tensile* or *elongational* or *Trauton's viscosity* for extension acting in the 1 - direction:

$$\zeta = \frac{\sigma_{11}}{\dot{\lambda}_{11}} \tag{III.23}$$

For zero extension rate, extensional viscosity reduces to $\zeta = 3\eta$.

For an incompressible, isotropic fluid, *normal stress difference* in the directions transverse to the flow direction may be defined as:

$$\sigma_{11} - \sigma_{22} = 2\,\eta\,(\dot{\gamma}_{11} - \dot{\gamma}_{22})$$

The stresses, strains, and rates of strain are identical in both transverse directions. Further,

$$\zeta = \frac{(\sigma_{11} - \sigma_{22})}{\lambda_{11}} \tag{III.24}$$

Equation III.24 is valid for extensional viscosity of an incompressible fluid, while for a solid there is a difference caused by the fact that $\sigma_{22} = 0$.

Under influence of stress or strain, some rearrangements on the molecular scale take place inside the material. These changes do require some finite time to occur. The time may be very short, almost infinitely short, or it may be long. If the rearrangements take infinitely much, or closely so, time we have purely elastic material; the energy invested in the material is stored. If the time for the molecular relocation is infinitely short we have purely viscous material; all the energy input is spent on overcoming the internal friction. Practically all real materials are viscoelastic as there are neither infinitely long nor infinitely short rearrangement times to be encountered. The relation between the time needed for the rearrangements and the time scale of the experiment may be described by the *Deborah number*:

$$N_D = \theta_{mat}/\theta_{exp} \tag{III.25}$$

Linear viscoelastic material is not characterized by a simple summation of the viscous and elastic behavior. Instead, the simplest constitutive equation for a viscoelastic body has the form of a linear differential equation of the form:

$$\sigma + a\, d\sigma/dt = b\gamma + c\, d\gamma/dt \tag{III.26}$$

III.2 Excitations and Responses

A more adequate representation of real materials requires differential equations containing higher derivatives of stress and strain. Behavior of some materials may be impossible to describe by linear equations, and the coefficients may not be constant. However, every material may be treated as linear if one considers it in terms of infinitesimal deformations. In practice, many materials show linear behavior over a fairly large interval of deformations; the strain, however, must remain below a certain limit, the value of which is a material property. If the response to a stimulus is to be linear, two conditions must be satisfied: 1^o – the increase in a stimulus must increase the response by the same factor, and 2^o – a sequence of stimuli must result in a response which is the sum of responses to the individual stimuli in the sequence. The general relation between the time dependent stress and strain is

$$\sum_{n=0}^{\infty} u_n \frac{d^n\sigma(t)}{dt_n} = \sum_{m=0}^{\infty} q_m \frac{d^m\varepsilon(t)}{dt_m} \tag{III.27}$$

u_n and q_m are constant coefficients. Equation III.27 may be put in the form of an linear differential operator equation, which is being used in the form of its Laplace transform

$$\bar{f}(s) = \int_0^{\infty} f(t)e^{-st}\, dt \tag{III.28}$$

where s is the transform variable.

If the strain at $t = 0$ is taken as the reference strain, then the one sided Laplace transformation may be used. In this way, the differential equation with constant coefficients in the *time domain* becomes an algebraic equation in the *complex domain*. Transformation of the operator equation gives

$$\bar{u}(s)\ \bar{\sigma}(s) = \bar{q}(s)\ \bar{\varepsilon}(s) \tag{III.29}$$

where $\bar{\sigma}(s)$ and $\bar{\varepsilon}(s)$ are transforms of stress and strain, respectively. Also,

$$\bar{u}(s) = \sum_n u_n s^n \qquad \text{and} \qquad \bar{q}(s) = \sum_m q_m s^m \tag{III.30}$$

represent polynomials of the variable of transforms. From equations III.29 and III.30 one obtains

$$\bar{\sigma}(s) = \bar{Q}(s)\bar{\varepsilon}(s) \qquad \text{and} \qquad \bar{\varepsilon}(s) = \bar{U}(s)\bar{\sigma}(s) \tag{III.31}$$

where

$$\bar{Q}(s) = \frac{\bar{q}(s)}{\bar{u}(s)} \qquad \text{and} \qquad \bar{U}(s) = \frac{\bar{u}(s)}{\bar{q}(s)} \tag{III.32}$$

Applying the nomenclature proposed by Tschoegl,[68] $\bar{Q}(s)$ and $\bar{U}(s)$ are called *operational relaxance* and *retardance*, respectively, in shear. The corresponding relations between stress and rate of strain are the *operational impedance* and *admittance*, respectively.

The operator equation (III.27) and its transform (equation III.28) represent one of the possible forms of the general constitutive equation for viscoelastic bodies. It describes the superposition of response to any chain of excitations. The additivity is essential to the linear behavior. In the time domain, these characteristics may be expressed in the form of *Boltzmann superposition integrals*:

$$\sigma(t) = \int_0^\infty Q(t-u)\ \varepsilon(u)\ du \tag{III.33}$$

$$\varepsilon(t) = \int_0^\infty U(t-u)\ \sigma(u)\ du \tag{III.33 a}$$

Due to commutativity of the convolution operation, equations III.33 may be also written as

$$\sigma(t) = \int_0^\infty Q(u)\ \varepsilon(t-u)\ du \tag{III.34}$$

$$\varepsilon(t) = \int_0^\infty U(u)\ \sigma(t-u)\ du \tag{III.34 a}$$

In equations III.33 u denotes the *historic time* and in III.34 it denotes the *elapsed time*. It is, however, immaterial whether stress is taken as excitation and strain as response, or *vice versa*. Equations III.31 represent Hooke's law for shear flow in the complex plane. In equation III.31, $\bar{\epsilon}(s)$ is the *excitation transform* and $\bar{\sigma}(s)$ is the *response transform*; in equation III.31a, the roles are reversed. "The response and excitation transforms are connected through the *respondances*, $Q(s)$ and $U(s)$, which may also be called *material transforms* because they embody the properties of the material."[1] Viscoelastic behavior is time dependent: it is governed by the role of time in the excitation function. Therefore, it is important to examine the material behavior under influence of different types of excitation functions. Figure III.3 presents four of the more important excitation functions:

1. impulse applied at the time zero with a very short time of duration;
2. step excitation, where the impulse remains constant from the time zero on;
3. slope excitation, with the impulse increasing at a constant rate;
4. harmonic excitation. The harmonic excitation is of particularly great importance for experimental purposes.

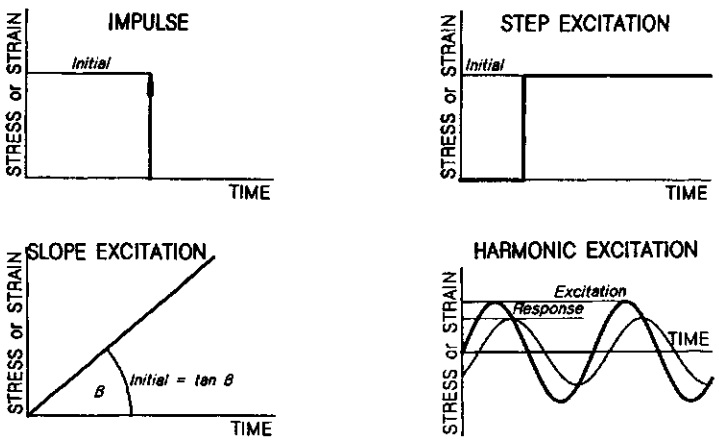

Figure III.3: *Different types of excitation functions.*

Strain impulse excitation may be presented as

$$\varepsilon(t) = \hat{\varepsilon}_0 \, \delta(t) \tag{III.35}$$

where $\delta(t)$ is the impulse or *delta function*:

$$\delta(t;\varepsilon) = (1/\pi) \int_0^\infty e^{-\varepsilon\omega} \cos(\omega t) \, d\omega = \frac{\varepsilon}{\pi(\varepsilon^2 + t^2)} \tag{III.36}$$

where ε may take any positive values. The function is bell shaped, with an increasing value of ε it becomes broader, but the integral of the function always

equals unity. If ε approaches zero, the bell shaped curve vanishes, and the height increases indefinitely:

$$\delta(t) = \frac{1}{\pi} \lim_{\varepsilon \to 0} \frac{\varepsilon}{(\varepsilon^2 + t^2)} \tag{III.37}$$

As described by equation III.37, the function $\delta(t) = \infty$ for $t = 0$, and $\delta(t) = 0$ for $t \neq 0$.

Laplace transformation gives

$$\bar{\varepsilon}(s) = \hat{e}_0 \tag{III.38}$$

After substitution into equation III.31, one obtains operational relaxance, and similarly operational retardance, respectively:

$$\bar{Q}(s) = \frac{\bar{\sigma}(s)}{\hat{\varepsilon}_0} \qquad \text{or} \qquad \bar{U}(s) = \frac{\bar{\varepsilon}(s)}{\hat{\sigma}_0} \tag{III.39}$$

where $\bar{\varepsilon}_0$ and $\bar{\sigma}_0$ are impulse strength, strain and stress, respectively. Retransformation of the equations gives

$$Q(t) = \frac{\sigma(t)}{\hat{\varepsilon}_0} \qquad \text{or} \qquad U(s) = \frac{\varepsilon(i)}{\hat{\sigma}_0} \tag{III.40}$$

The relaxance represents the response of the material to a unit impulse of strain, and retardance represents the response to a unit impulse of stress. The strain and stress, as functions of time, become respectively:

$$\sigma(t) = \int_0^t Q(t-u)\ \varepsilon(u)\ du = \int_0^t Q(u)\ \varepsilon(t-u) du \tag{III.41}$$

$$\varepsilon(t) = \int_0^t U(t-u)\ \sigma(u)\ du = \int_0^t U(u)\ \sigma(t-u)\ du \tag{III.42}$$

Step excitation is very widely used for experimental purposes. A mathematical description of it may be obtained from the integral of the delta function as ε tends to zero. The equation is

$$\begin{aligned} h(t) &= 0.5 + \frac{1}{\pi} \lim_{\varepsilon \to 0} \arctan(t/\varepsilon) = \\ &= 0.5 + \frac{1}{\pi} \lim_{\varepsilon \to 0} \int_0^\infty \exp(-\varepsilon\omega)\ \frac{\sin(\omega t)}{\omega}\ d\omega \end{aligned} \tag{III.43}$$

The delta function may be considered a derivative of the step function: $\delta(t) = dh(t)/dt$. The step function is $h(t) = 0$ for $t < 0$ and $h(t) = 1$ for $t > 0$.
The excitation function may be taken as

$$\varepsilon(t) = \varepsilon_0 \, h(t) \tag{III.44}$$

The Laplace transform of III.44, $\bar{\varepsilon}(s) = \varepsilon_0/s$ together with the Hooke's law, gives

$$\bar{\sigma}(s) = \frac{\bar{Q}(s)}{s} \, \varepsilon_0 \tag{III.45}$$

$\bar{Q}(s)/s$ is the transform of the modulus connecting time dependent stress with a unit step of strain. Consequently, after combining with equation III.45 and retransformation, one obtains:

$$G(t) = \frac{\sigma(t)}{\varepsilon_0} = \int_0^t Q(u) \, du \tag{III.46}$$

where $G(t)$ is the *shear relaxation modulus.*

Analogously, we may write the relationships for the shear strain response to a unit step stress, σ_0.

$$J(t) = \frac{\varepsilon(t)}{\sigma_0} = \int_0^t U(u) \, du \tag{III.47}$$

where $J(t)$ is *creep compliance* in shear. $G(0)$ and $J(0)$ represent the *instantaneous modulus* and *instantaneous compliance*, respectively.

Inversion of the Laplace transform of equation III.46 leads to four different forms of the relationship, in which $G(0)$ has been substituted with G_g - glassy modulus, respectively *glassy compliance* .

$$\sigma(t) = G_g \, \varepsilon(t) - \int_0^t \frac{dG(t-u)}{du} \, \varepsilon(u) \, du \tag{III.48}$$

$$\sigma(t) = G_g \, \varepsilon(t) - \int_0^t \frac{dG(u)}{du} \, \varepsilon(t-u) \, du \tag{III.48 a}$$

$$\sigma(t) = \int_0^t G(t-u) \, d\varepsilon(u) \tag{III.48 b}$$

$$\sigma(t) = \int_0^t G(t) \, \frac{d\varepsilon(t-u)}{du} \, du \tag{III.48 c}$$

$$\varepsilon(t) = J_g\ \sigma(t) - \int_0^t \frac{dJ(t-u)}{du}\ \sigma(u)\ du \tag{III.49}$$

$$\varepsilon(t) = G_g\ \sigma(t) - \int_0^t \frac{dJ(u)}{du}\ \sigma(t-u)\ du \tag{III.49 a}$$

$$\varepsilon(t) = \int_0^t J(t-u)\ d\sigma(u) \tag{III.49 b}$$

$$\varepsilon(t) = \int_0^t J(t)\ \frac{d\sigma(t-u)}{du} du \tag{III.49 c}$$

The *slope excitation* (see Figure III.3) means application of excitation which is growing at a constant rate, hence the other name *constant rate of stress (or strain) excitation.* In this type of excitation the limit of linear behavior of the material may be easily exceeded; the given solutions would, naturally, loose their validity.

If one denotes constant rate of strain as $\dot{\varepsilon}_0$ and constant rate of stress as $\dot{\sigma}_0$, then for a constant rate of strain is

$$\varepsilon(t) = \dot{\varepsilon}_0\ p(t) = \dot{\varepsilon}_0\ t \tag{III.50}$$

where $p(t)$ is the slope function, which is derived from the step function (equation III.43):

$$p(t) = t\ h(t) \tag{III.51}$$

For $t < 0$ $p(t) = 0$ and for $t > 0$ $p(t) = t$.
Laplace transformation of equation III.50 gives

$$\bar{\varepsilon}(s) = \dot{\varepsilon}_0/s^2 \tag{III.52}$$

and substitution into equation III.31 results in

$$\bar{\sigma}(s) = \frac{\bar{Q}(s)}{s^2}\ \dot{\varepsilon}_0 \tag{III.53}$$

$\bar{\sigma}(s)/\dot{\varepsilon}_9 = \bar{\eta}(s)$ represents the transform of time dependent *shear viscosity.* In effect, one obtains

$$\bar{\eta}(s) = \frac{\bar{Q}(s)}{s^2} = \frac{\bar{G}(s)}{s} = \eta(t) = \frac{\sigma(t)}{\dot{\varepsilon}_0} \tag{III.54}$$

The further relationships are:

$$\eta(t) = \frac{\sigma(t)}{\dot{\varepsilon}_0} = \int_0^t G(u)\ du = \int_0^t \int_0^v Q(u)\ \ du\ dv \tag{III.55}$$

$$\bar{Q}(s) = s\bar{G}(s) = s^2\ \bar{\eta}(s) \tag{III.56}$$

And from retransformation:

$$Q(t) = \frac{dG(t)}{dt} + G(0)\ \delta(t) = \frac{d^2\eta(t)}{dt^2} + \eta'(0)\ \delta(t) + \eta(0)\ \delta'(t) \tag{III.57}$$

$$G(t) = \frac{d\eta(t)}{dt} + \eta(0)\ \delta(y) \tag{III.58}$$

Equations for the response to constant rate of stress are analogous to those given for the response to the constant rate of strain.

Steady state *harmonic* or *sinusoidal* excitation (Figure III.4) is often used in testing. The sequence of reasoning is similar as for previous cases.[1] Harmonic strain excitation may be expressed mathematically as

$$\varepsilon(t) = \varepsilon_0\ [\sin(\omega t) + i\cos(\omega t)] = \varepsilon_0\ \exp(i\omega t) \tag{III.59}$$

In this case, ε_0 means strain amplitude and ω is frequency in radians. This is the general equation for sinusoidal curves, and in this case describes the *generalized harmonic strain* (or *stress*).

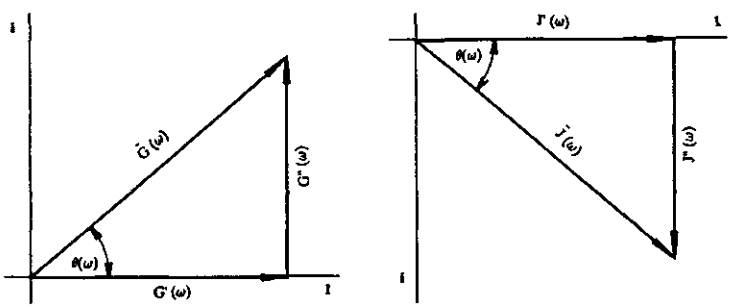

Figure III.4: *Vector resolution of complex modulus and complex compliance; modulus or storage compliance.*

Again, the process of deriving the equations is similar. The Laplace transform of the response to $\varepsilon(t)$ is

$$\bar{\varepsilon}(s) = \frac{\varepsilon_0}{s - i\,\omega} \tag{III.60}$$

After substitution to equation III.31 one obtains

$$\bar{\sigma}(s) = \frac{\varepsilon_0\ \bar{Q}(s)}{s - i\,\omega} \tag{III.61}$$

After retransformation to the real time axis, the total response obtained consists of two parts: 1^o – a steady state response in the form of a periodic function resulting from the poles of excitation, and 2^o – a nonperiodic transient response arising from the poles of the material transforms, $Q(s)$ and $U(s)$. For steady state, it is then

$$\frac{\bar{\sigma}_{ss}(s)}{\varepsilon_0} = \frac{\bar{Q}(i\,\omega)}{s - i\,\omega} \tag{III.62}$$

$$\sigma_{ss} = \bar{Q}(i\omega)\varepsilon_0 \, e^{i\omega t} \tag{III.63}$$

In this case, the response varies with frequency ω, which for steady state is of primary interest, rather than time. Consequently, one may denote $\varepsilon(\omega) = \varepsilon_0 \exp(i\omega t)$ and change the equations accordingly.

The quantity $\bar{Q}(i\omega)$ has the dimensions of modulus, and in polymer rheology is usually denoted $G^*(\omega)$ and called *complex shear modulus*, but it may also be called *harmonic relaxance*.

In analogy to the above, one may derive the *harmonic retardance* or *complex shear compliance*, $J^*(\omega)$.

$$\varepsilon_{ss}(t) = \bar{U}(i\omega)\sigma_0 e^{i\omega t} \tag{III.64}$$

$$J^*(\omega) = \bar{U}(s)|_{s=i\omega} \tag{III.65}$$

The complex nature of the modulus in compliance permits each of them to be decomposed into either Cartesian or polar coordinates:

$$G^*(\omega) = G'(\omega) + iG''(\omega) = \bar{G}(\omega) \, e^{i\theta(\omega)} \tag{III.66}$$

$$J^*(\omega) = J'(\omega) - iJ''(\omega) = \bar{J}(\omega) \, e^{-i\theta(\omega)} \tag{III.67}$$

$G'(\omega)$ and $J'(\omega)$ are proportional to the energy stored during a cycle of deformation in a unit of volume of a material and are called *storage modulus* and *storage compliance*, respectively. $G''(\omega)$ and $J''(\omega)$ are proportional to the energy dissipated per unit of volume of the material and are called *loss modulus* or *loss compliance*; $\theta(\omega)$ is *loss angle*. As may be seen from Figure III.4 the following relationships are self understood:

$$\bar{G}(\omega) = \{[G']^2 + [G''(\omega)]^2\}^{\frac{1}{2}} \tag{III.68}$$

$$\bar{J}(\omega) = \{[J']^2 + [J''(\omega)]^2\}^{\frac{1}{2}} \tag{III.68 a}$$

$$\tan\theta(\omega) = \frac{G''(\omega)}{G'(\omega)} = \frac{J''(\omega)}{J'(\omega)} \tag{III.69}$$

$$G'(\omega) = \bar{G}(\omega) \, \cos\theta(\omega) \tag{III.70}$$

$$G''(\omega) = \bar{G}(\omega) \, \sin\theta(\omega) \tag{III.70 a}$$

$$J'(\omega) = J(\omega) \, \cos\theta(\omega) \tag{III.71}$$

$$J''(\omega) = \bar{J}(\omega) \, \sin\theta(\omega) \tag{III.71 a}$$

$$\bar{G}(\omega) = \frac{\sigma_0(\omega)}{\varepsilon_0} \qquad \text{and} \qquad \bar{J}(\omega) = \frac{\varepsilon_0(\omega)}{\sigma_0} \tag{III.72}$$

Absolute modulus and compliance represent the ratio of the response amplitude to the excitation amplitude. The loss angle represents the phase difference of the response and excitation, the stress always reaches its peak before strain does.

The further relationships of interest are:

$$\dot{\varepsilon}(t) = d\varepsilon(t)/dt = -\varepsilon_0 \, \omega[\sin(\omega t) - i\cos(\omega t)] \tag{III.73}$$

$$\varepsilon(\omega) = \varepsilon_0(\omega)\ \exp\{i[\omega t - \theta(\omega)]\} \tag{III.74}$$

$$\varepsilon_0(\omega)\ \cos\theta(\omega) = \sigma_0\ J'(\omega) \tag{III.75}$$

$$\varepsilon_0(\omega)\ \sin\theta(\omega) = \sigma_0\ J''(\omega) \tag{III.75 a}$$

$$\dot{\varepsilon}(\omega) = d\varepsilon(\omega)/dt = i\omega\varepsilon(\omega) \tag{III.76}$$

$$\eta^*\ \omega = \frac{\sigma(\omega)}{i\omega\varepsilon(\omega)} = \frac{G^*(\omega}{i\omega} \tag{III.77}$$

$$G(t)\ \frac{\sigma(t)}{\varepsilon_0} = \mathcal{L}^{-1}\frac{\bar{\mathrm{Q}}(\mathrm{s})}{\mathrm{s}} = \int_0^{\mathrm{t}} \mathrm{Q(u)\ du} \tag{III.78}$$

$$\eta(t)\ \frac{\sigma(t)}{\varepsilon_0} = \mathcal{L}^{-1}\frac{\bar{\mathrm{Q}}(\mathrm{s})}{\mathrm{s}^2} = \int_0^{\mathrm{t}} \mathrm{G(u)\ du} \tag{III.79}$$

$$G^*(t) = \frac{\sigma(\omega)}{\varepsilon(\omega)} = [\bar{Q}(s)]_{s=i\omega} \tag{III.80}$$

$$J(t) = \frac{\varepsilon(t)}{\sigma_0} = \mathcal{L}^{-1}\frac{\bar{\mathrm{U}}(\mathrm{s})}{\mathrm{s}} \tag{III.81}$$

$$\chi(t) = \frac{\varepsilon(t)}{\dot{\sigma}_0} = \mathcal{L}^{-1}\frac{\bar{\mathrm{U}}(\mathrm{s})}{\mathrm{s}^2} \tag{III.82}$$

$$J^*(t) = \frac{\varepsilon(\omega)}{\sigma(\omega)}\ [\bar{U}(s)]_{s=i\omega} \tag{III.83}$$

III.3 Mechanical Models

It has been found convenient to represent material properties by mechanical models. The common symbols used for this purpose are presented in Figure III.5. The *spring* represents idealized storage of elasticity, without any losses to friction; E represents operational *elastance*, which is the proportionality coefficient for the relation between force, f, and displacement, x, or velocity, v. The *dashpot* represents idealized energy dissipation as heat, with no energy storage involved. *Frictance*, F, is the proportionality constant for the relation between force and constant velocity at which the two ends of the dashpot are moving. Kinetic energy may be represented by *mass*, which responds to applied force with pure inertia, with no energy storage or dissipation. The coefficient of proportionality between force and the resulting acceleration is called *inertance*. These relationships may be put in a mathematical form as follows:

Potential energy storage:

$$\bar{f}(s) = E\ \bar{x}(s) \tag{III.84}$$

Dissipation of energy:

$$\bar{f}(s) = F\ s\ \bar{x}(s) \tag{III.84 a}$$

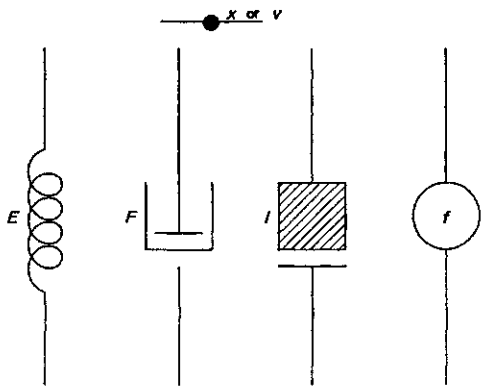

Figure III.5: *Symbols used in mechanical rheological models: E - for elastance of the spring, F - for frictance of the dashpot, I - for inertance of the mass, f - applied force, x - displacement, v - velocity.*

Storage of kinetic energy:

$$\bar{f}(s) = I\ s^2\ \bar{x}(s) \qquad (III.84\,b)$$

If the system is at rest, then:

$$x(0) = \dot{x}(0) = \ddot{x}(0) \equiv 0 \qquad (III.84\,c)$$

where the dots denote differentiation *versus* time.

The relaxances are additive, so

$$\bar{f}(s) = (I\,s^2 + Fs + E)\ \bar{x}(s) = Q_t(s)\ \bar{s} \qquad \text{(III.85)}$$

After retransformation of equation III.85 one obtains

$$f(t) = I\ \frac{d^2x(t)}{dt^2} + F\ \frac{dx(t)}{dt} + E\ s(t) \qquad \text{(III.86)}$$

The rules to be observed in the model analysis are:

- *relaxances add in parallel*
- *retardances add in series.*

These rules result from the fact that forces add in parallel and displacements add in series. In a parallel combination of the passive elements, all elements are displaced equally, then the forces in the elements are additive. In a series combination, the same force acts through all the elements, therefore the displacements are additive.

In cases of rotational motion, the transform of force is replaced by the transform of torque, $\bar{M}(s)$; the transform of the linear displacement is replaced by the transform of angular displacement, $\bar{\theta}(s)$. Consequently, the respondances change correspondingly: inertance to the moment of inertia, frictance to the moment of mechanical resistance, elastance to the moment of stiffness. The reciprocal of elastance is mechanical compliance, the reciprocal of frictance is called, μ, glidance.

In modeling rheological behavior the rheological respondances are translated to mechanical respondances by use of a *shape factor*, b. In this way, force and displacement (or torque and angular displacement) are converted to stress and strain.

$$\frac{\sigma}{\varepsilon} = b_t \frac{f}{x} = b_r \frac{M}{\theta} \tag{III.87}$$

Here b_t has the dimension of reciprocal length and b_r has the dimension of reciprocal volume. Thus, instead of force, displacement (or velocity), elastance and frictance we use stress, strain (or rate of strain), modulus, viscosity, respectively. Inertivity is usually omitted since it has negligible effect, except for cases involving high frequencies or impact, and then it is represented by the density of the material.

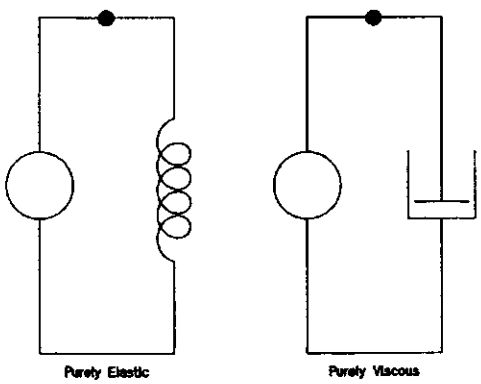

Figure III.6: *Models of purely elastic and purely viscous behavior.*

Figure III.6 exemplifies how purely elastic and purely viscous materials may be modeled using simple elements. One may write

$$\bar{\sigma}(s) = G\ \bar{\varepsilon}(s) \tag{III.88}$$

for the model of purely elastic, and

$$\bar{\sigma}(s) = \eta\ \bar{s}\ \varepsilon(s) = \eta\dot{\bar{\varepsilon}}\ (s) \tag{III.89}$$

for the model of purely viscous behavior. The models and equations III.88 and III.89 represent the equations III.1 and III.2. If one considers equation III.31, then it becomes evident that the relaxance, $Q(s)$, is G - the shear modulus. From equation III.89 and III.31 one may see that $\bar{Q}(s)$ is ηs. Both G and η are the model parameters. Per analogy, J and ϕ/s are operational retardances. For better visualization, all the quantities are gathered in table III.1.

Viscoelastic behavior may be represented in the simplest way by the Voigt or by the Maxwell model (Figure III.7). In the parallel Voigt model, all of the elements have the same strain and the stresses are additive.

$$\bar{Q}(s) = G + \eta\ s \tag{III.90}$$

Table III.1
Overview of Respondances.

Model Parameter	Operational Respondance	Harmonic Respondance
G	G	G
J	J	J
η	ηs	$i\omega\eta$
(ϕ)	ϕ/s	$\phi/i\omega$

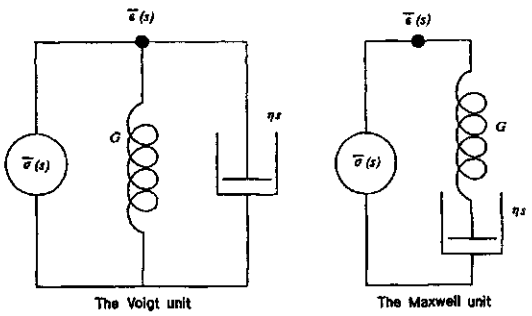

Figure III.7: *The simplest models of viscoelastic behavior: the Voigt unit and the Maxwell unit.*

and further

$$\bar{\sigma}(s) = (G + \sigma s)\ \bar{\varepsilon}(s) \tag{III.91}$$

which is a Laplace transform of the equation

$$\sigma = G\,\varepsilon + \eta\,\frac{d\varepsilon}{dt} \tag{III.92}$$

Equation III.92 is a simple combination of equations for purely elastic and purely viscous response. The retardance of the Voigt model is

$$\bar{U}_v(s) = \frac{J}{1 + \tau_v s} \tag{III.93}$$

where τ is *retardation time*, $\tau = J/\phi$, and $\phi = 1/\eta$.

The Maxwell arrangement of dash-pot and spring in a series may be described as

$$\bar{U}(s) = J + \frac{\phi}{s} \tag{III.94}$$

where $J = 1/G$ and $\phi = 1/\eta$. Furthermore

$$\bar{E}(s) = \left(J + \frac{\phi}{s}\right)\bar{\sigma}(s) \tag{III.95}$$

The differential equation which corresponds to III.95 is

$$\frac{d\varepsilon}{dt} = \frac{1}{\eta}\,\sigma + \frac{1}{G}\,\frac{d\sigma}{dt} \tag{III.96}$$

The relaxance of the Maxwell model is

$$\bar{Q}_M(s) = \frac{G\,\theta_M\,s}{1+\theta_M\,s} \tag{III.97}$$

where θ_M is *relaxation time*, $\theta_M = \eta/G$. With the help of relaxation and retardation times, one may write the equation for operational retardance of the Maxwell model

$$\bar{U}_M(s) = J + \left(\frac{\phi}{s}\right) = J\left(1 + \frac{1}{\theta_M\,s}\right) \tag{III.98}$$

and for the operational relaxance of the Voigt model

$$\bar{Q}_v(s) = G + \eta s = G\,(1+\theta_v s) \tag{III.99}$$

Real viscoelastic materials behave neither like the Maxwell nor like the Voigt model: they behave rather like some kind of combination of both models. A real viscoelastic material shows relaxation of stress, as well as a retardation of strain, depending on the kind of excitation. The delay in behavior reflects the time needed for the material to adjust to the changes forced upon it – it is easy to imagine this fact on the molecular level.

The meaning of the relaxation time becomes quite clear if one substitutes equation III.97 into equation III.45 and inverts the transform, which leads to

$$\sigma(t) = \varepsilon_0\,G\,\exp\left(\frac{-t}{\theta_m}\right) \tag{III.100}$$

Equation III.100 describes stress in a Maxwell unit when subjected to a constant strain of ε_0. Since $G\varepsilon_0 = \sigma_0$, the initial magnitude of stress, one therefore obtains

$$\sigma(t) = \sigma_0\,\exp\left(\frac{-t}{\theta_m}\right) \tag{III.101}$$

The initial stress relaxes exponentially with time. For a perfectly elastic material, the initial stress ought to remain constant for an indefinite time. For a perfectly viscous material the relaxation time ought to be zero.

From equation III.101 results that

$$t(\theta_M) = \sigma_0/e = 0.369\,\sigma_0. \tag{III.102}$$

In a similar way, one may substitute equation III.93 into $\bar{\varepsilon}(s) = \bar{U}(s)\sigma_0/s$ and retransform it to obtain

$$\varepsilon(t) = \sigma_0\,J\,\left[1 - \exp\left(\frac{-t}{\theta_v}\right)\right] \tag{III.103}$$

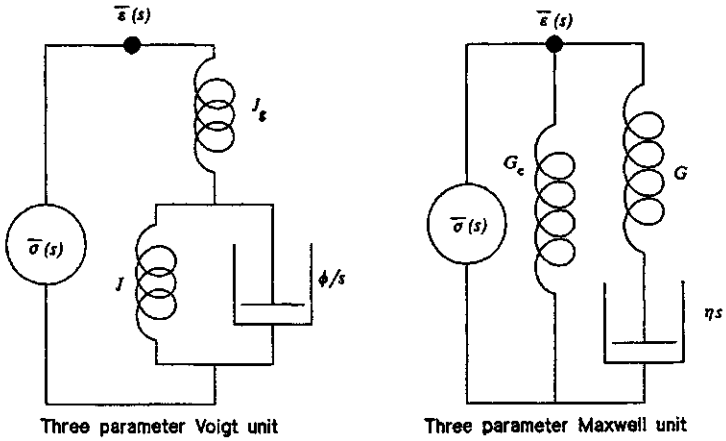

Figure III.8: *Three-parameter Voigt and Maxwell models.*

Equation III.103 describes strain as a function of the time that has elapsed since the stress σ_0 was applied. $J\sigma_\infty = \varepsilon_\infty$, the final strain at $t = \infty$. For $t = \theta_v$ $\varepsilon(\theta_v) = 0.631\ \varepsilon_\infty$.

In order to better describe the actual properties of a viscoelastic material, many units of both Maxwell and Voigt variety may be joined in different combinations. In fact, any of the constitutive equations derived in the past in different ways may be described by such combinations. In this highly abridged description of the rheological problems are quoted only simple examples: three parameter models of Voigt and of Maxwell.

Combinations of the different units make sense only when units of different kind are joined in the system. Figure III.8 shows such "expansions" of the unitary models previously considered. The Voigt model has been obtained by addition of a spring in series with a basic Voigt unit. The retardance of the model may be obtained using equation III.93 and the combination principle:

$$\bar{U}_v(s) = J_g + \frac{J}{1+\theta s} \tag{III.104}$$

$J/\phi = \theta$ is the retardation time of the model. For the step input one may obtain

$$\bar{\varepsilon}(s) = \sigma_0 + \left[\frac{J_g}{s} \times \frac{J}{s\,(1+\theta s)}\right] \tag{III.105}$$

and after retransformation

$$\varepsilon(t) = \sigma_0 \left\{J_g + J \left[1 - \exp\left(\frac{-t}{\theta}\right)\right]\right\} = \varepsilon_0 + \varepsilon \left[1 - \exp\left(\frac{-t}{\theta}\right)\right] \tag{III.106}$$

If a constant stress is applied, according to this model, there is an instantaneous strain, $\varepsilon_0 = J_g\sigma_0$, after which follows a delayed strain to reach an equilibrium value, $\varepsilon_e = \varepsilon_0 + \varepsilon = J_e\sigma_0$ at $t = \infty$. This kind of behavior is called *creep*, and

$J(t) = \varepsilon(t)/\sigma_0$ is called *creep compliance.* J_g is the instantaneous compliance (at $t = 0$), and J_e is the equilibrium compliance (at $t = \infty$), $J_e = J_g + J$. J is delayed (retarded) compliance.

Considering the three-element Voigt model under step strain, one may take advantage of the relation $Q(s)U(s) = 1$ and the defining relationship of equilibrium compliance to obtain

$$\bar{Q}_v(s) = \frac{1 + \theta s}{J_e + J_g \theta s} \tag{III.107}$$

and for a constant strain the stress transform is

$$\bar{\sigma}(s) = \varepsilon_0 \frac{1 + \theta s}{s\ (J_e + J_g \theta s)} \tag{III.108}$$

After inversion of the transform one obtains

$$\sigma(t) = \varepsilon_0 \left[\frac{1}{J_e} + \frac{J_e - J_g}{JeJg}\right] = \sigma_e + \sigma \exp\left(\frac{-t}{\theta'}\right) \tag{III.109}$$

where

$$\tau' = \frac{J_g\ \theta}{J_e} \tag{III.110}$$

The initial stress in response to a step strain is

$$\bar{\sigma}(0) = \sigma\ \varepsilon_e + \sigma = \varepsilon_0 \left[\frac{1}{J_e} + \frac{J_e - J_g}{J_e J_g}\right] = \frac{\varepsilon_0}{J_g} \tag{III.111}$$

If $t = \infty$, according to this model, the material relaxes to an equilibrium value of $\sigma_e = \varepsilon_0/J_e$.

If one considers the Maxwell model with an added parallel spring (Figure III.8), then the relaxance is

$$\bar{Q}_M(s) = G_e + \frac{G\ \theta\ s}{1 + \theta\ s} \tag{III.112}$$

Relaxances add in parallel, so for a step strain of magnitude ε_0 the Laplace transform is

$$\bar{\sigma}(s) = \varepsilon_0 \left(\frac{G_e}{s} + \frac{G\ \theta}{1 + \theta\ s}\right) \tag{III.113}$$

After inversion of the transform, one obtains

$$\sigma(t) = \varepsilon_0\ \left[G + G \exp\left(\frac{-t}{\theta}\right)\right] = \sigma_e + \sigma\ \exp\left(\frac{-t}{\theta}\right) \tag{III.114}$$

At $t = 0$, the stress is $\sigma_0 = \sigma_e + \sigma = G_g \varepsilon_0$, and the instantaneous modulus is

$$G_g = G_e + G \tag{III.115}$$

In the last equation G_e is *equilibrium modulus* and G is *relaxing modulus.* If $t = \infty$ then $\sigma_e = G_e \varepsilon_0$. The behavior is identical with the three-element Voigt model.

The three-parameter Maxwell model responds to a step stress as the Voigt model does, and the mathematical formalism is completely analogous. The three element models describe properties of solids (*arrheodictic*, cross linked polymers with equilibrium strain), while properties of liquids (*rheodictic*, where strain increases linearly with time, and there is no equilibrium value) are described better by four- parameter models.

Respondances are rational algebraic functions (polynomials) of complex transform variables. These functions have poles

$$\bar{U}_v(s) = \frac{\bar{u}_v(s)}{\bar{q}_v(s)} \quad \bar{Q}_M(s) = \frac{\bar{q}_M(s)}{\bar{u}_M(s)} \tag{III.116}$$

which are the roots of the polynomials in the denominators, $\bar{q}_v(s)$ and $\bar{u}_M(s)$. The roots of the numerators are equal zero. In this way the zeros of retardances are the poles of the relaxances and *vice versa*. This results from the fact that $U(s)Q(s) = 1$. The Voigt and Maxwell units have no zeros, therefore they are not real models.

For the rheodictic materials, and those include practically all fiber forming polymers, retardance must have a pole in the origin of the axes, while relaxances have a zero at the same point. For arrheodictic materials the situation is reversed. When the pole and zero locations are known, the respondances are fully determined.

Real polymers only in rare cases may be approximately described by three or four-element models. Generalized models (Figures III.9 and III.10) have been developed to fit the real polymers. Nevertheless, detailed description of the real polymers are better. However, a detailed description of the mathematical derivations would greatly exceed the boundaries of this book; hence, the reader is referred to the specialistic, original source.[1] Only some of the final equations will be quoted here.

Summation of a number of Maxwell units results in the generalized Maxwell - Wiechert model, the relaxance of which is

$$\bar{Q}(s) = \sum_{n=0}^{N-1} \frac{G_n\ \theta_n\ s}{1 + \theta_n\ s} \tag{III.117}$$

The corresponding relaxation modulus is:

$$G(t) = \sum_{n=0}^{N-1} G_n \exp\left(\frac{-t}{\theta_n}\right) \tag{III.118}$$

The relaxance may be interpreted as a superposition of exponentials representing some unitary processes. This model represents rheodictic materials; to obtain a description of arrheodictic materials, it is necessary to replace the spring and dashpot unit in the zero position of the Maxwell model with a spring of G_e. This

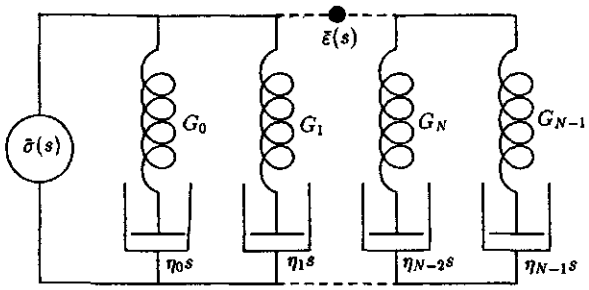

Figure III.9: *Generalized Maxwell - Wiechert model for the description of rheodictic material behavior.*

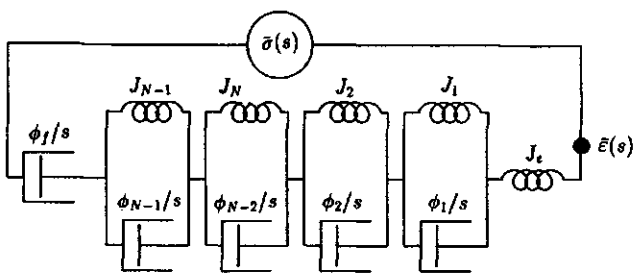

Figure III.10: *Generalized Voigt-Kelvin model for the description of rheodictic material behavior.*

new model would have the relaxance

$$\bar{Q}(s) = G_e + \sum_{n=1}^{N-1} \frac{G_n\ \theta_n\ s}{1 + \theta_n\ s} \tag{III.119}$$

It is important to stress that for the rheodictic materials, the summation in equations III.117 and III.118, as well as in others to follow, is carried out from zero to $N-1$ (consult also Figure III.9). In the case of arrheodictic descriptions, the summation needs to be carried from 1 to $N-1$, as the spring of G_e occupies the zero position.

The complex modulus of a rheodictic material is

$$G^*(\omega) = \sum_{n=0}^{N-1} \frac{G_n\ i\ \omega\ \theta_n}{1 + i\ \omega\ \theta_n} \tag{III.120}$$

The storage modulus equation is

$$G'(\omega) = \sum_{n=0}^{N-1} \frac{G_n\ \omega^2\ \theta_n^2}{1 + \omega^2\ \theta_n^2}. \tag{III.121}$$

For the loss modulus the equation is

$$G''(\omega) = \sum_{n=0}^{N-1} \frac{G_n\ \omega\ \theta_n}{1 + \omega\ \theta_n}. \tag{III.122}$$

It is necessary to stress that for the cases involving arrheodictic materials, the summations in equations III.120 through III.122 must be carried from $n = 1$ to $N - 1$. On integration of equation III.120 one obtains:

$$\eta(t) = \{G_e\}t + \sum_n G_n\ \theta_n\ \left[1 - \exp\left(\frac{-t}{\theta_n}\right)\right] =$$

$$= \{G_e\}\ t + \eta_{\{f\}} - \sum_n \eta_n\ \exp\left(\frac{-t}{\theta_n}\right) \tag{III.123}$$

The values in braces, for example $\{G_e\}$, concern arrheodictic behavior and for rheodictic behavior are to be omitted. Further,

$$\eta_{\{f\}} = \sum_n \eta_n = \sum_n G_n\ \theta_n \tag{$III.123\,a$}$$

is the sum of the viscosities of all dashpots, and is usually written simply as η. For rheodictic cases the sum represents the steady flow viscosity, η_f.

The generalized Wiechert model is often named the Kelvin model or Wiechert - Kelvin model, and for rheodictic behavior it is presented in Figure III.10. For arrheodictic behavior the dashpot, ϕ_f/s, is omitted. To avoid presentation of the equations separately for rheodictic and for arrheodictic materials, braces will be used for those terms which are to be omitted in the case of rheodictic behavior, e.g. $\{\phi_f/s\}$. This is opposite to the case of the generalized Maxwell model, where arrheodictic terms are put in braces. The retardance of such models may be presented in two different forms III.124 and III.124a:

$$\bar{U}(s) = J_g + \sum_{n=1}^{N-1} \frac{J_n}{1 + \theta_n\ s} + \left\{\frac{\phi_f}{s}\right\} \tag{III.124}$$

$$\bar{U}_\bullet(s) = J_e^{\{o\}} - \sum_{n=1}^{N-1} \frac{J_n\ \theta_n\ s}{1 + \theta_n\ s} + \left\{\frac{\phi_f}{s}\right\} \tag{$III.124\,a$}$$

It is necessary to note that the two forms of retardances are equivalent, $U(s) = U_\bullet(s)$, the notation is to indicate the origin of the different forms.

The creep compliance of the generalized Voigt model is

$$J(t) = J_g + \sum_n J_n\ \left[1 - \exp\left(\frac{-t}{\theta_n}\right)\right] + \{\phi_f\ t\} \tag{III.125}$$

or

$$J_\bullet(t) = J_e^{\{o\}} - \sum_n J_n\ \exp\left(\frac{-t}{\theta_n}\right) + \{\phi_f\ t\} \tag{$III.125\,a$}$$

The complex compliance is

$$\bar{J}^*(\omega) = J_g + \sum_{n=1}^{N-1} \frac{J_n}{1 + i\,\omega\,\theta_n} + \left\{ \frac{\phi_f}{i\,\omega} \right\} \tag{III.126}$$

or

$$\bar{J}^*_{\bullet}(\omega) = J_e^{\{o\}} - \sum_{n} \frac{J_n\, i\,\omega\,\theta_n}{1 + i\,\omega\,\theta_n} + \left\{ \frac{\phi_f}{i\,\omega} \right\} \tag{$III.126\,a$}$$

The real and imaginary compliances are, respectively

$$\bar{J}'(\omega) = J_g + \sum_{n=1}^{N-1} \frac{J_n}{1 + [\omega^2\,\theta_n^2]} \tag{III.127}$$

or

$$\bar{J}_{\bullet}(\omega) = J_e^{\{o\}} - \sum_{n} \frac{J_n\,\omega^2\,\theta_n^2}{1 + \omega^2\,\theta_n^{*2}} \tag{$III.127\,a$}$$

$$\bar{J}''(\omega) = \sum_{n=1}^{N-1} \frac{J_n\,\omega\,\theta_n}{1 + \omega^2\,\theta_n^2} + \left\{ \frac{\phi_f}{\omega} \right\} \tag{III.128}$$

The loss modulus has only one form, equation III.128.

The properties described by the equations III.117 through III.128 imply that a material has more than one relaxation or retardation time. The set of relaxation or retardation times may consist of several points, it may have many points to form a *discrete* spectrum, or it may also be taken as a *continuous spectrum.* The summation present in equations III.117 through III.128 suggest also than each time, θ_n, is associated with a modulus, G_n. One may then speak about a spectrum of moduli *versus* time, and, consequently, one may take modulus as *strength of a spectrum.* In a similar way, compliance may be taken as the strength of retardation spectrum. The pairs of G_n and n may be grouped and the groups treated as single relaxation time.

Experimental data may be fit into the model equations; there are several methods of doing so described in the literature on rheology.[1,2]

The fundamental equations of viscoelastic behavior (equations III.30 and III.31) may be described in a more generalized way: *response transform equals material transform multiplied by excitation transform.*[1] Since the excitation and response are clearly connected to time (or frequency), the material functions are also time dependent. However, for every imaginable driving function, there exists a different material function. To avoid the inconvenience of multiplicity of material functions a material response function has been introduced under the name *spectral distribution function* or just *relaxation spectrum.* There are relaxation spectra derived from response to strain, retardation spectra derived from response to stress. There may be line (or discrete) spectra or continuous, spectra *versus* time or *versus* frequency. Due to its fundamental importance, representation of the response function in the form of spectra is termed the *canonical representation.*

The generalized equation III.119 describing a discrete spectrum may be changed to describe a continuous relationship:

$$\bar{Q}(s) = \{G_e\} + \int_0^\infty \hat{Q}(\theta)\ \frac{\theta s}{1+\theta\ s}\ d\theta \tag{III.129}$$

where $\hat{Q}(\theta)$ is a continuous function of the relaxation time, θ, and its integral replaces the sum of the discrete points G_n. The $Q(\theta)$ function is also called the *distribution of relaxation times.* The function has dimensions of modulus divided in time; it is the density of modulus per time. The *relaxation spectrum* – with the dimensions of modulus, in a common notation, may be given as

$$\hat{G}(\theta) = H(\theta) = \theta\ \hat{Q}(\theta) \tag{III.130}$$

If the new function (equation III.130) is introduced into equation III.129 one obtains:

$$\bar{Q}(s) = \{G_e\} + \int_{-\infty}^\infty H(\theta)\ \frac{\theta s}{1+\theta\ s}\ d\ln\theta \tag{III.131}$$

The term $d\ln$ represents a conventional term which strictly formally ought to be written as $d\theta/\theta$; should this correct term be used, then the lower integration limit must be *zero.*

Other important relationships may be given as follows:

$$G(t) = \{G_e\} + \int_{-\infty}^\infty H(\theta)\ \exp\left(\frac{-t}{\theta}\right)\ d\ \ln\ \theta \tag{III.132}$$

$$G^*(\omega) = \{G_e\} + \int_{-\infty}^\infty H(\theta)\ \frac{i\ \omega\ \theta}{1+i\ \omega\ \theta}\ d\ \ln\ \theta \tag{III.133}$$

$$G'(\omega) = \{G_e\} + \int_{-\infty}^\infty H(\theta)\ \frac{\omega^2\ \theta^2}{1+\omega^2\ \theta^2}\ d\ln\theta \tag{III.134}$$

$$G''(\omega) = \int_{-\infty}^\infty H(\theta)\ \frac{\omega\ \theta}{1+\omega^2\ \theta^2}\ d\ln\theta \tag{III.135}$$

$$\eta(t) = \{G_e t\} + \int_{-\infty}^\infty \theta\ H(\theta)\ \left[1-\exp\left(\frac{-t}{\theta}\right)\right]\ d\ln\theta \tag{III.136}$$

As far as corresponding equations for the *retardation time spectrum* from the creep behavior are concerned, there is a full analogy to all the above.

$$\bar{U}(s) = J_g + \int_0^\infty \hat{U}(\theta)\ \frac{1}{1+\theta\ s}\ d\theta\ + \left\{\frac{\phi_f}{s}\right\} \tag{III.137}$$

We introduce $\hat{J}(\theta)$, a continuous function of the retardation time, θ, and when its integral replaces the sum of the discrete points, the resulting $J(\theta)$ function is called the *distribution of retardation times.* Other remarks are analogous to those for the relaxation function. Common notation gives

$$\hat{J}(\theta) = L(\theta) = \theta\ \hat{U}(\theta) \tag{III.138}$$

If the function (equation III.138) is introduced into equation III.137 one obtains:

$$\bar{J}(s) = \frac{J_g}{s} + \int_{-\infty}^{\infty} L(\theta)\ \frac{1}{s\ (1+\theta\ s)}\ d\ \ln\theta + \left\{\frac{\phi_f}{s^2}\right\} \tag{III.139}$$

The term $d\ln\theta$ represents a conventional term which strictly formally ought to be written as $d\theta/\theta$; should this correct term be used, then the lower integration limit must be zero.

Other important relationships may be given as follows:

$$J(t) = J_g + \int_{-\infty}^{\infty} L(\theta)\ \left[1 - \exp\left(\frac{-t}{\theta}\right)\right]\ d\ \ln\theta + \{\phi_f\ t\} \tag{III.140}$$

$$J^*(\omega) = J_g + \int_{-\infty}^{\infty} L(\theta)\ \frac{1}{1+i\ \omega\ \theta}\ d\ln\theta + \left\{\frac{\phi_f}{i\ \omega}\right\} \tag{III.141}$$

$$J'(\omega) = J_g + \int_{-\infty}^{\infty} L(\theta)\ \frac{1}{1+\omega^2\ \theta^2}\ d\ln\theta \tag{III.142}$$

$$J''(\omega) = \int_{-\infty}^{\infty} L(\theta)\ \frac{\omega\ \theta}{1+i\ \omega\ \theta}\ d\ln\theta + \left\{\frac{\phi_f}{i\ \omega}\right\} \tag{III.143}$$

$$\chi(t) = \{J_e t\} - \int_{-\infty}^{\infty} \theta\ L(\theta)\ \left[1 - \exp\left(\frac{-t}{\theta}\right)\right]\ d\ln\theta + \frac{\{\phi_f\}\ t^2}{2} \tag{III.144}$$

In effect, experimental response functions are integrals over the continuous spectral distribution functions multiplied by the kernel functions specific to the time regime of the stimulus. Every given value of a response function depends on all the values of the spectral function from $\theta = 0$ to $\theta = \infty$. The experimental response functions are called *functionales.*

The relaxation and retardation spectra may also be expressed as functions of *relaxation (retardation) frequencies*, which are reciprocals of the corresponding times. The frequency functions form the basis for computation of the time spectra from the experimental response functions. Exact solutions of mathematical problems involved in the spectra calculation are known, however, they are rarely used,

not only due to their complexity, but also because of their sensitivity to input data inaccuracies. Approximate methods are most often used instead. Many different computational procedures to obtain both continuous and discrete point spectra are known. Description of all these methods greatly exceeds the main topic of this book, so the reader must be referred to the specific literature on the subject.[1–6], though, to some extent, we shall return to this subject in chapter IV.

For a long time it has been suspected[34,64] that relaxation functions may be affected by stress and/or strain to which the material is subjected. As the time progresses, there is more and more evidence, both theoretical and experimental, published[72&ref.] that it is indeed the case.

As it is evident from the above given canonical equations of the experimental response functions, a number of time independent material constants are included in the equations. Here, the constants, and their interrelations, are summarized. Equilibrium shear modulus

$$G_e = \lim_{s\to 0} \bar{Q}(s) = \lim_{t\to\infty} G(t) = \lim_{\omega\to 0} G'(\omega) \tag{III.145}$$

Glassy shear modulus

$$G_g = \lim_{s\to\infty} \bar{Q}(s) = \lim_{t\to 0} G(t) = \lim_{\omega\to\infty} G'(\omega) \tag{III.146}$$

Steady state (rheodictic) or equilibrium shear compliance

$$\begin{aligned} J_e^{\{o\}} &= \lim_{s\to 0} \left[\bar{U}(s) - \{\phi_f/s\}\right] = \\ &= \lim_{t\to\infty} \left[J(t) - \{\phi_f\ t\}\right] = \\ &= \lim_{\omega\to\infty} J'(\omega) \end{aligned} \tag{III.147}$$

Glassy shear compliance

$$J_g = \lim_{s\to\infty} \bar{U}(s) = \lim_{t\to 0} J(t) = \lim_{\omega\to\infty} J'(\omega) \tag{III.148}$$

Steady state shear fluidity

$$\phi_f = \lim_{s\to 0} s\ \bar{\phi}(s) = \lim_{t\to\infty} \phi(t) = \lim_{\omega\to\infty} \phi'(\omega) \tag{III.149}$$

Steady state shear viscosity

$$\eta_f = \lim_{s\to 0} s\ \bar{\eta}(s) = \lim_{t\to\infty} \eta(t) = \lim_{\omega\to\infty} \eta'(\omega) \tag{III.150}$$

III.4 Energy Considerations

It is important to note the energy questions connected to material deformation. In line with the brevity of this overview, only those relationships are quoted which

are most relevant to fiber formation processes. And so, for strain excitation – stress relaxation in step excitation cases the energy stored, $W_s(t)$, due to imposition of an initial strain, ε_0, is

$$W_s(t) = \left(\frac{\varepsilon_0^2}{2}\right)\left[\{G_e\} + \int_{-\infty}^{\infty} H(\theta)\ \exp\left(\frac{-2\ t}{\theta}\right)\ d\ln\theta\right] \tag{III.151}$$

The rate of energy storage, $\dot{W}_s(t)$, is

$$\dot{W}_s(t) = \varepsilon_0^2\left[G_g\ \delta\ (2\ t) - \int_{-\infty}^{\infty} \theta^{-1}\ H(\theta)\ \exp\left(\frac{-2\ t}{\theta}\right)\ d\ln\theta\right] \tag{III.152}$$

The energy dissipated, $W_d(t)$, under the same conditions may be described as

$$W_d(t) = \left(\frac{\varepsilon_0^2}{2}\right)\int_{-\infty}^{\infty} H(\theta)\ \left[1 - \exp\left(\frac{-2\ t}{\theta}\right)\right]\ d\ln\theta \tag{III.153}$$

The rate of energy dissipation, $\dot{W}_d(t)$, is

$$\dot{W}_d(t) = \varepsilon_0^2 \int_{-\infty}^{\infty} \theta^{-1}\ H(\theta)\ \exp\left(\frac{-2\ t}{\theta}\right)\ d\ln\theta \tag{III.154}$$

For creep behavior, stress excitation - strain retardation with step excitation, for a continuous retardation spectrum (continuous distribution of retardances) the stored energy, $W_s(t)$, is

$$W_s(t) = \left(\frac{\sigma_0^2}{2}\right)\left\{J_g + \int_{-\infty}^{\infty} L(\theta)\ \left[1 - \exp\left(\frac{-2\ t}{\theta}\right)\right]\ d\ln\theta\right\} \tag{III.155}$$

The corresponding rate of energy storage, $\dot{W}_s$, is

$$\dot{W}_s(t) = \frac{\sigma_0^2}{2}\left\{J_g(t) + 2\int_{-\infty}^{\infty} \theta^{-1}\ L(\theta)\left[1 - \exp\left(\frac{-2t}{\theta}\right)\right]\exp\left(\frac{-t}{\theta}\right) d\ln\theta\right\} \tag{III.156}$$

The dissipated energy, $W_d(t)$, under the same conditions is

$$W_d(t) = \left(\frac{\sigma_0^2}{2}\right)\left\{\int_{-\infty}^{\infty} L(\theta)\ \left[1 - \exp\left(\frac{-2\ t}{\theta}\right)\right]\ d\ln\theta + 2\ t\{\phi_f\}\right\} \tag{III.157}$$

The rate of energy dissipation, $\dot{W}_d(t)$, in accordance with the above, is formulated as

$$\dot{W}_d(t) = \sigma_0^2 \times \left[\int_{-\infty}^{\infty} \theta^{-1} \, L(\theta) \, \exp\left(\frac{-2\,t}{\theta}\right) \, d\ln\theta + \{\phi_f\} \right] \tag{III.158}$$

The total energy is, of course, the sum of the stored and dissipated energies.

III.5 Uniaxial Extension

The majority of the rheology issues covered above concerns shear stresses. Uniaxial extension (or compression) is at least as important, or even more so, in fiber formation and other areas (e.g. testing). The matrices of the transforms of stress and strain tensors for this case are:

$$|\bar{\sigma}_{ij}| = \begin{vmatrix} \bar{\sigma}_{11} & 0 & 0 \\ 0 & 0 & 0 \\ 0 & 0 & 0 \end{vmatrix} \tag{III.159}$$

$$|\bar{\gamma}_{ij}| = \begin{vmatrix} \bar{\gamma}_{11} & 0 & 0 \\ 0 & \bar{\gamma}_{22} & 0 \\ 0 & 0 & \bar{\gamma}_{33} \end{vmatrix} \tag{III.160}$$

From these tensors one can derive the following relationships:

$$\bar{\sigma}_{11}(s) = 2\,\bar{Q}(s)\,[\bar{\gamma}_{11}(s) - \bar{\gamma}_{22}(s)] \tag{III.161}$$

or

$$\bar{\sigma}_{11}(s) = 2\,s\,\bar{G}(s)\,[\bar{\gamma}_{11}(s) - \bar{\gamma}_{22}(s)] \tag{III.162}$$

From the last equations it follows that the shear modulus is known if the stress in transverse direction is known. Experimentally, however, it is very difficult to determine the transverse stress and to overcome this, the ratio of stress to strain is used instead. In the transform plane, the *stretch relaxance*, $\bar{Y}$, and *elongational (stretch) relaxation modulus*, $\bar{E}$, become

$$\frac{\bar{\sigma}_{11}(s)}{\bar{\gamma}_{11}(s)} = \bar{Y}(s) = s\,\bar{E}(s) \tag{III.163}$$

The canonical representations of the relaxance are

$$\bar{Y}(s) = \{E_e\} + \int_{-\infty}^{\infty} H_E(\theta) \, \frac{\theta\,s}{1+\theta\,s} \, d\ln\theta \tag{III.164}$$

$$\bar{Y}_{\bullet}(s) = E_g - \int_{-\infty}^{\infty} H_E(\theta) \, \frac{1}{1+\theta\,s} \, d\ln\theta \tag{III.165}$$

Here $H_E(\theta)$ is *elongational (or tensile, or stretch) modulus*, E_e and E_g are correspondingly *equilibrium* and *glassy elongational modulus* .

It is very important to stress that $H_E(\theta)$ is similar to the shear relaxation spectrum, but that there are fundamental differences in the relaxation behavior between the two.

The transform of the canonical equation of elongational viscosity may be presented as

$$\bar{Y}(s) = \frac{\bar{E}(s)}{s} = \frac{\{E_e\}}{s^2} + \int_{-\infty}^{\infty} H_E(\theta) \frac{\theta\, s}{1+\theta\, s}\, d\ln\, \theta \tag{III.166}$$

This leads to the expression for extensional viscosity analogous to equation III.136

$$\zeta(t) = \{E_e\ t\} + \int_{-\infty}^{\infty} \theta H_E(\theta) \left[1 - \exp\left(\frac{-t}{\theta}\right)\right] d\ln\theta \tag{III.167}$$

In considering compliance, by definition the *elongational retardance* is $\bar{L}(s) = 1/\bar{Y}(s)$ and the *elongational compliance* is $sD(s) = 1/E(s)$ and, by analogy with equation III.155, they may be presented as

$$\frac{\bar{\gamma}_{11}(s)}{\bar{\sigma}_{11}(s)} = \bar{L}(s) = s\,\bar{D}(s) \tag{III.168}$$

And further

$$\bar{L}(s) = E_g + \int_{-\infty}^{\infty} L_D(\theta) \frac{1}{1+\theta s}\, d\ln\ \theta + \left\{\frac{1}{\zeta_f\, s}\right\} \tag{III.169}$$

$$\bar{L}_{\bullet}(s) = D_e^{\{o\}} - \int_{-\infty}^{\infty} L_D(\theta) \frac{\theta\, s}{1+\theta\, s}\, d\ln\theta + \left\{\frac{1}{\zeta_f\, s}\right\} \tag{III.170}$$

$L_D(\theta)$ is the *elongational retardation spectrum*, D_g, and $D_e^{\{o\}}$ are the glassy and *pseudo-equilibrium compliance*, and ζ_f is the *steady state elongational viscosity.*

As mentioned above

$$H_E(\theta) \neq H(\theta) \neq H_K(\theta) \qquad \text{and} \qquad L_D(\theta) \neq L(\theta) \neq L_K(\theta) \tag{III.171}$$

The constants in equations III.169 and III.170 may be defined as

$$\int_{\infty}^{\infty} H_E(\theta)\, d\ln\theta = E_g - \{E_e\} \tag{III.172}$$

$$\int_{-\infty}^{\infty} L_D(\theta)\, d\ln\theta = D_e^{\{o\}} - D_g \tag{III.173}$$

If a material is subjected to uniaxial strain in any direction, the two remaining directions also display certain strain. The ratio of the lateral strain to the excitation strain is known as *Poisson's ratio.* While for purely elastic materials Poisson's ratio is a material constant, for viscoelastic materials Poisson's ratio is a time dependant function. If the undeformed material is isotropic, then the contraction in the two lateral directions is identical. Poisson's ratio is the same, irrespective of the type of excitation (stress or strain). A stretched material experiences stress relaxation in the strain direction but the transverse strain is delayed; it reaches its final value after infinite time. The strain retardation makes the problem analogous to compliance, so we have

$$\bar{\nu}s = \mu_g + \sum_{n=1}^{N-1} \mu_n \frac{1}{1+\theta_n\, s} = \mu_e - \sum_{n=1}^{N-1} \mu_n \frac{\theta_n\, s}{1+\theta_n\, s} \tag{III.174}$$

$$\bar{\mu}s = \frac{\mu_g}{s} + \sum_{n=1}^{N-1} \mu_n \frac{1}{s\,(1+\theta_n\, s)} = \frac{\mu_e}{s} - \sum_{n=1}^{N-1} \mu_n \frac{\theta_n}{1+\theta_n\, s} \tag{III.175}$$

In equations III.174 and III.175 $\bar{\nu}$ and $\bar{\mu}$ are analogous to $\bar{U}$ and $\bar{J}$. In this case θ is called *delay time*, as it is not identical with retardation time in tension. The glassy and equilibrium Poisson's ratios are designated respectively as μ_g and μ_e, and $\sum_n \mu_n = \mu_e - \mu_g$.

By its nature, Poisson's ratio is arrheodictic and it may have maximum value of -0.5 for ideally incompressible material at equilibrium. The glassy Poisson's ratio is normally smaller than 0.5, mostly closer to $\frac{1}{3}$.

The canonical representation of Poisson's ratio function may be derived by obtaining a spectrum of delay times, $m(\theta)$, analogously to the above given cases for Voigt model.

The final equations are:

$$\mu(t) = \mu_g + \int_{-\infty}^{\infty} m(\theta)\, [1 - \exp(-t/\theta)]\, d\ln\theta \tag{III.176}$$

$$\mu(t) = \mu_e + \int_{-\infty}^{\infty} m(\theta)\, \exp(-t/\theta)\, d\ln\theta \tag{III.177}$$

III.6 Extrudate Swelling

There is a phenomenon of particular importance to fiber formation: *die swell* or Barus effect or extrudate swelling. Namely, if a material is extruded from a capillary of a given diameter, the diameter of the extrudate almost always is larger than the diameter of the capillary used. This phenomenon is somewhat elusive; the available explanation appears incomplete, and the problem is certainly

very complex. Empirical observations indicate that die swell depends strongly on the capillary length (or aspect ratio) and on the rate of shear in the capillary.[7,8] Influence of these parameters on die swell may be appreciated from figures III.11, III.14. and III.15. These types of influences led to the belief that die swell is related to the melt elasticity,[9] to the relaxational processes. Further, it has been proved that die swell depends also on the extensional flow component developed at the entry to the capillary.[10,13]

V.Cogswell[11] relates die swell, B, to the recoverable strain, ε_R, as follows:

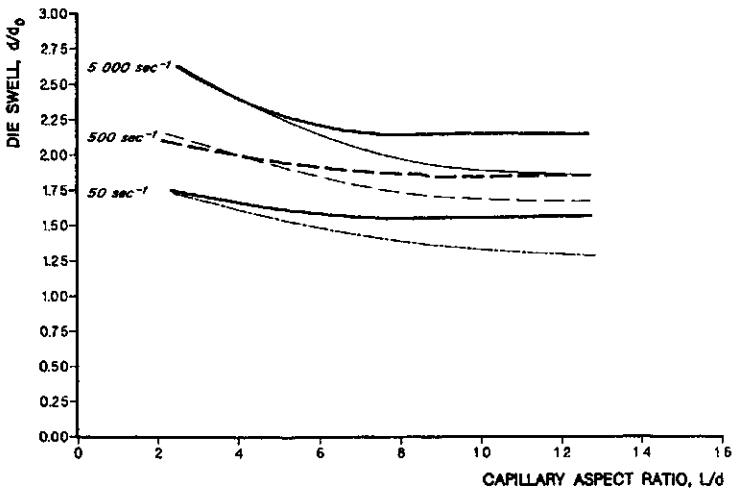

Figure III.11: *The relationship between die swell, defined as the ratio of the extrudate diameter over capillary diameter, and the angle of the capillary entrance cone: heavy lines* 60°, *fine lines* 20°. *After Walczak*[12]

$$\varepsilon_R = \ln B^2 \tag{III.178}$$

For the case of free convergence at the die entry, the extensional stress, σ_E, may be calculated from the relationship:

$$\sigma_E = \sigma_s / \tan\varphi \tag{III.179}$$

where φ is one half of the entry cone angle, σ_s is shear stress corresponding to the shear rate $\dot{\gamma} = 4Q/\pi r^3$ for the cone location, if the shear stress - shear rate relationship is known. Otherwise, there are approximate formulae for the extension rate:[14]

$$\dot{\varepsilon} = \left(\frac{\dot{\gamma}}{4}\right)\left[\frac{\sin^3\varphi}{(1-\cos\varphi)}\right] = \left(\frac{\dot{\gamma}}{2}\right)\sin\varphi\ \left[\frac{(1-\cos\varphi)}{2}\right] \tag{III.180}$$

and another:[11,13]

$$\dot{\varepsilon} = \left(\frac{\dot{\gamma}}{2}\right)\ \tan\varphi \tag{III.181}$$

Both of the above equations have been developed for Newtonian flow. The equation for non-Newtonian fluids developed by Cogswell[11] requires the knowledge of the local pressure drop, P_0, during extrusion, as well as the exponent in the power law equation, n, on which the derivation is based:

$$\dot{\varepsilon} = \frac{4\ \sigma_s}{[3\ (n+1)P_0]} \tag{III.182}$$

For the flow in conical ducts (entry to a capillary), the fluid velocity at the wall is zero, maximum velocity is in the center. In effect the flow velocity profile includes telescopic shear and elongation. Again, there is a disagreement as to the final formulation of extension rate in the Newtonian flow. Similarly as for the free convergence, all the suggested solutions become identical for the cone angle approaching zero. The only non-Newtonian solution is given by Cogswell:[11]

$$\dot{\varepsilon} = \left[\frac{3n+1}{n+1}\right] \times \left(\frac{\dot{\gamma}}{2}\right) \times \tan\varphi \tag{III.183}$$

Here n is the exponent in the power law equation $\sigma_s \propto \dot{\gamma}^n$. For Newtonian fluids, when $n = 1$, equation III.183 becomes

$$\dot{\varepsilon}_{max} = \dot{\gamma}\ \tan\varphi \tag{$III.183\,a$}$$

Die swell is the result of the superposition of the recoverable part of the extensional strain and of the expansion created by the normal shearing force facing cessation of the capillary wall restraint. The second reason was demonstrated by Zidan[15], in full agreement with the experimental work published by Goren and Wronski[16,17] and by Gavis and Madon[18], that even Newtonian fluids show extrudate expansion at Reynolds numbers below 16, while at higher Reynolds numbers the extrudate diameter is smaller than the capillary radius. Figures III.12 and III.13 present calculated flow patterns and velocity distribution in the vicinity of the capillary exit for Newtonian fluid with different ratios of wall friction coefficient, f, over viscosity, $\omega = f/2\eta$.

The die swell descriptions given above do not unite all the aspects of the phenomenon. The problem is even further complicated by the fact that die swell depends quite strongly on the shearing history of the polymer. This may be seen from the comparison given in Figure III.14, which represents the same polymer as obtained from polymerization in a powder form (top of figure) and after pelletization in a screw extruder with no degradation detectable analytically (bottom of figure). The only speculative explanation for this dependence, as nebulous as it may be, may be the change in the molecular entanglements leading to changes in the elastic response. The polymer history cannot be quantified yet. Die swell, as important as it is in fiber formation processes, still remains elusive and not fully defined.

It has been found that extensional viscosity (Trouton viscosity) may be best described in relation to tensile stress. It initially is equal to $3\eta_0$ (where η_0 is zero shear

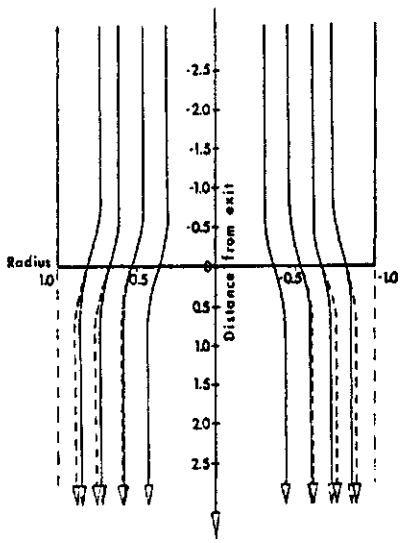

Figure III.12: *Streamlines in flow of Newtonian fluid in the vicinity of the capillary exit; negative values in the capillary, positive values outside the capillary. Parameter:* $\omega = 0.5$ *full drawn lines,* $\omega = 0.05$ *dashed lines. After Zidan.*[15]

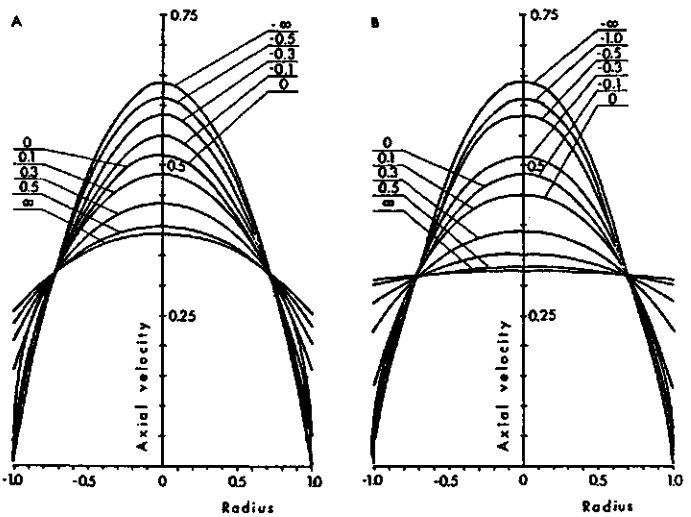

Figure III.13: *Velocity profiles in the vicinity of capillary exit, as calculated for Newtonian fluid. Parameter: distance from capillary (negative inside the capillary). A for* $\omega = 0.5$*, B for* $\omega = 0.05$*. After Zidan.*[15]

viscosity), and increases with increasing stress,[15,19,20] contrary to shear viscosity which decreases with increasing stress. The increase of extensional viscosity with stress continues to about $10^5 Pa$,[20] (ranging from $6.68 \cdot 10^5 Pa$ to $2.15 \cdot 10^5 Pa$[21]), thereafter the viscosity may become constant, and later decreases. The decrease

of viscosity with stress is responsible for flow instabilities, both in the capillary flow due to the extensional flow component, and in extensional flow as such.

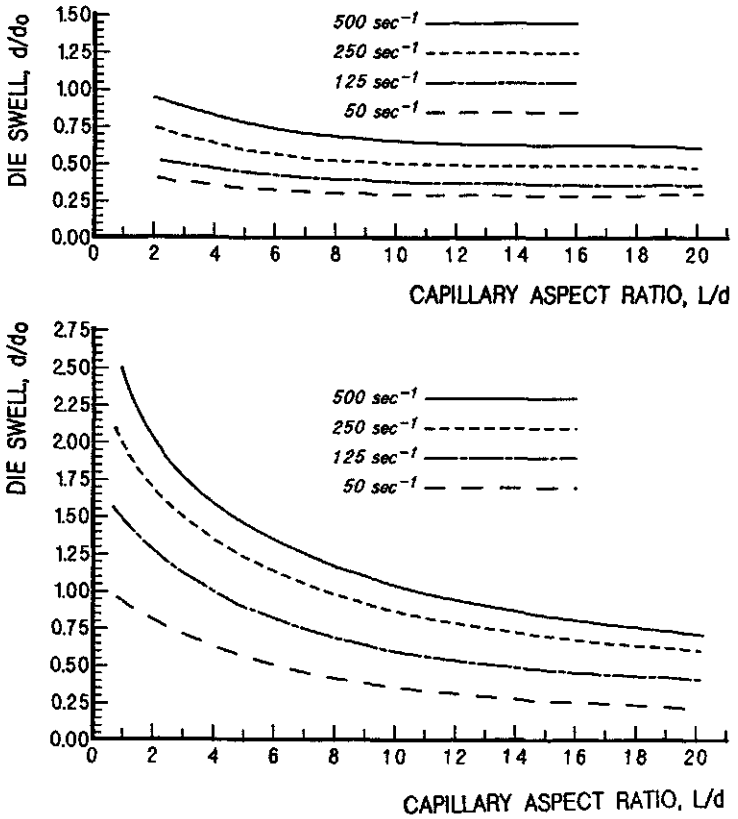

Figure III.14: *Die swell, $B = r/r_0$, in relation to the capillary aspect ratio, l/d; parameter shear rate. Top: polypropylene in powder form, "as polymerized", bottom: the same polymer as above but pelletized in a screw extruder.*[12]

In general, any rheological function in one mode may be obtained from data acquired in another mode if the two functions are available. For example, one may obtain the bulk relaxance in isotropic compression from data obtained in shear experiments. One may obtain information on shear flow from data obtained in uniaxial extension. Nevertheless, as an exception, information on extensional flow cannot be extracted from data obtained in other modes of deformation. It is unfortunate, as experimentally analyses of extensional flow are very difficult and are usually burdened with a larger error.

It appears important to mention, however, the simplified method of obtaining information on extensional flow from experiments with converging flow. Cogswell[28] postulated that the flow from a reservoir into a zero-length capillary represents a sum of a shear and extensional component. The suggested solutions were based on the power law constitutive equation. Bersted[29] substituted the power law

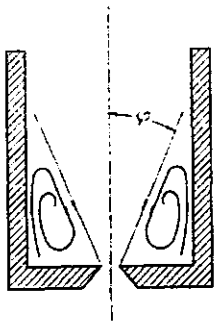

Figure III.15: *Schematic representation of the flow pattern at the entry to a capillary.*

equation, $\tau \propto \dot{\gamma}^n$, with a more "flexible" formula:

$$\eta = \frac{\eta_0}{1 + A\,\dot{\gamma}^{\frac{2}{3}}} \tag{III.184}$$

and the exponent, n, is

$$n = \frac{1 + \left(\frac{A\,\dot{\gamma}^{2/3}}{3}\right)}{(1 + A\,\dot{\gamma}^{\frac{2}{3}})} \tag{III.185}$$

where η_0 is zero-shear viscosity and $\dot{\gamma}$ is shear rate. In effect, the original Cogswell and the modified equations form the following set which describes the process: Pressure drop due to extension at any point of the cone:

$$P_E(h) = \left[\frac{\zeta \tan\varphi(h)}{3}\right] \quad [\dot{\gamma}(h-1) - \dot{\gamma}(h)] \tag{III.186}$$

Here, ζ is extensional viscosity, φ is one half of the angle of the entrance cone and $\tan\varphi = (2\eta/\zeta)^{1/2}$, h is the location in relation to the conical duct exit. Figure III.15 shows schematically the polymer flow in the vicinity of capillary entry. The vortices formed around the more or less conical flow pattern are the reason for the pattern development, unless the entry has conical walls to serve the same purpose. Pressure drop due to shear at any point of the cone:

$$P_S(h) = \frac{2\,\eta_0\,\dot{\gamma}(h-1)\,[1 - \Gamma^{n(h)}]}{3\,\tan\varphi(h)\,\left\{1 + \frac{[A\dot{\gamma}^{2/3}(h-1)]}{3}\right\}} \tag{III.187}$$

where $\Gamma = \dot{\gamma}(h)/\dot{\gamma}(h-1)$. The summaric pressure drop at any point is

$$P(h) = 2\,\sqrt{P_S(h)\,P_E(h)} \tag{III.188}$$

Total pressure drop is

$$P = \sqrt{\frac{8\,\eta_0\,\zeta}{9}} \times \Xi \tag{III.189}$$

where

$$\Xi = \left\{ \sum_{h=2}^{m} \frac{\dot{\gamma}(h-1)\,[\dot{\gamma}(h-1) - \dot{\gamma}(h)]\,(1-\Gamma)^{n(h)}}{\left(1 + \frac{[A\ \dot{\gamma}(h-1)^{2/3}]}{3}\right)} \right\}^{\frac{1}{2}} \tag{III.190}$$

Average extension rate is

$$\langle \dot{\varepsilon} \rangle = \frac{\dot{\gamma}_1}{2} \left\{ \frac{2\,\eta_0}{\zeta_1\,[1 + A\ \dot{\gamma}(1)^{2/3}]} \right\}^{\frac{1}{2}} \tag{III.191}$$

After rearranging equation III.189, extensional viscosity becomes

$$\zeta = \left(\frac{9}{8}\right) \left(\frac{P}{\Xi}\right)^2 \times\ \eta_0^{-1} \tag{III.192}$$

Change of the constitutive equation improves the agreement between the data calculated from conical capillary experiments and those obtained by direct measurements of extensional viscosity only insignificantly. As a next step improvement, Bersted[29] uses extensional viscosity as a function of extension rate instead of Cogswell's constant "average extensional viscosity" in equation III.186. Cogswell's equation for extension rate function in a conical capillary is

$$\varepsilon(h) = \tan\varphi(h)\ \left[\frac{2\,Q}{\pi r(h)^3}\right] \tag{III.193}$$

Further, it is assumed that

$$\begin{aligned} \zeta(h) \quad &= \zeta(h-1) \left[\tfrac{\dot{\varepsilon}(h)}{\dot{\varepsilon}(h-1)}\right]^{k(h)} \quad = \\ &= \zeta(h-1) \left[\tfrac{r(h)^3}{r(h-1)^3}\right]^{3k(h)} \quad = \\ &= \zeta(h-1) \left[\tfrac{\dot{\gamma}(h)}{\dot{\gamma}(h-1)}\right]^{k(h)} \end{aligned} \tag{III.194}$$

Finally, the pressure drop function due to extension is

$$\begin{aligned} P_E(h) \quad &= \quad \frac{\zeta(1)\tan\varphi(h)}{3[1+k(h)]} \times \left\{ \dot{\gamma}(h-1)\left[1 - \Gamma^{1-k(h)}\right] \times \right. \\ &\times \quad \left. \left[\frac{\dot{\gamma}(h-1)}{\dot{\gamma}(h-2)}\right]^{k(h-1)} \cdots \left[\frac{\dot{\gamma}(2)}{\dot{\gamma}(1)}\right]^{k(1)} \right\} \end{aligned} \tag{III.195}$$

The summaric pressure drop function of height h is

$$\begin{aligned} P(h) = \Bigg\{ &\left[\frac{8Q(h)}{3}\right] \left[\frac{\zeta(h)\dot{\gamma}(h-1)}{3+3k(h)}\right] \times \left[1 - \Gamma^{n(h-1)}\right] \times \\ &\times \left[1 - \Gamma^{1+k(h)}\right] \left[\frac{\dot{\gamma}(h-1)}{\dot{\gamma}(h-2)}\right]^{k(h-1)} \cdots \left[\frac{\dot{\gamma}(2)}{\dot{\gamma}(1)}\right]^{k(2)} \Bigg\}^{\frac{1}{2}} \end{aligned} \tag{III.196}$$

where

$$Q(h) = \frac{\eta_0 \, \dot{\gamma}(h-1)}{[1 + A \, \dot{\gamma}(h-1)^{2/3}]} \qquad (III.196\,a)$$

At the capillary exit ($h = 1$) the extensional viscosity is

$$\zeta = (P/\Xi)^2 \qquad (III.197)$$

In this case Ξ becomes

$$\Xi = \sum_{h=1}^{m} \left\{ \left(\frac{8 \, \eta_0 \, \dot{\gamma}(h-1)^2}{[9(1 + A \, \dot{\gamma}(h-1)^{2/3}]/3} \right) \times \right.$$

$$\left. \times \left[1 - \Gamma^{n(h-1)}\right] \left[1 - \Gamma^{1+k(h)}\right] \right\}^{\frac{1}{2}} \times Z(h) \qquad (III.197\,a)$$

where

$$Z(h) = \left\{ \frac{1}{[1 + k(h)]} \right\} \times \left[\frac{\dot{\gamma}(h-1)}{\dot{\gamma}(h-2)} \right]^{k(h-1)} \cdots \left[\frac{\dot{\gamma}(2)}{\dot{\gamma}(1)} \right]^{k(2)} \qquad (III.197\,b)$$

The above given calculations are rather involved, so it is obvious a computer has to be employed for their execution. Further, the value of $k(h)$ is not known *a priori*, and it probably varies with the extension rate. Consequently, the entire problem must be solved iteratively by employing equations III.184 through III.191 as the first approximation, and subsequently the extensional viscosity as a function of the extension rate is improved by fitting the data into equations III.196.[29] The agreement between the data so calculated and the results obtained from experimental determination of extensional viscosity is quite good for several polymers, however, for narrow molecular weight polystyrenes, the agreement is disappointing. In summary, experimental determination of extensional flow is to be recommended over the above given method of calculation. Nevertheless, the Cogswell and Bersted work seems important as it points to rather interesting phenomena taking place during extrusion through capillaries with conical entrance.

The work of Cogswell and Bersted has been extended further by J. R. Collier and co-workers.[66,67] These authors find that extensional flow data may be obtained from extrusion through hyperboloidal - conical dies ("capillaries"). The experiments may be conducted either by an axial coextrusion of two polymers with largely different viscosities (by a factor of 30 to 100)[66] or even without the "lubricating" polymer.[67]

Interesting investigations of die swell were reported by Tanner and co-workers.[60,61] Some of their key findings may be summarized as follows:

- For Newtonian fluids the maximum diameter of the extrudate is attained only 0.5 diameters below the exit of the capillary. This is true for non-Newtonian fluids at Weissenberg number of 1 ($Wi = \theta v/R$ where θ - relaxation time, $\bar{v}$ - average axial velocity, R - capillary diameter).

- Extrudate swelling is strongly dependent on both elasticity and cooling.
- Presence of a yield stress in a material strongly reduces the swelling.

In the end, one must conclude that the swelling problem is extremely complex and despite all the interesting work done thus far, a firm understanding and prediction ability still seem to lie in the future.

III.7 Flow Instability in Extrusion

Flow instabilities had been observed for a long time,[22–24] and many different theories have been put forth to explain it. It has been noticed that the onset of flow instabilities coincides with the Deborah number approaching one,[25,26] and this is understood as an indication that the instability is related to the viscoelastic nature of the fluid. Also, an interesting thermodynamic explanation of the flow instabilities has been offered,[27] and this is in agreement with the understanding that the flow instability is a phenomenon resulting from the viscoelastic nature of the polymer.

The recent two decades have brought more convincing interpretations of the phenomenon. During extrusion through a capillary, the necessary pressure requirement to drive the extrusion increases with the increasing flow rate. Nevertheless, the relationship is not as simple as it might result from the basic equations for flow in tubular ducts (capillaries). Figure III.16 shows the general relationship between pressure in the barrel of a capillary rheometer and polymer flow rate.[57–59] The graph is divided into five regions:

I – where extrudate is smooth and at constant flow, pressure is constant with time,

II – where extrudate has a more or less rough surface ("shark skin"), though pressure is constant with time,

III – where flow is unstable, uneven, spurting exit of polymer while pressure has a "saw tooth" relation with time,

IV – large deformations of extrudate: uneven diameter, spiral, "porous surface" and pressure mostly constant with time.

V – behavior very similar to that in region IV.

Hatzikiriakos[57] believes that the critical factor in formation of the "shark skin" is acceleration of the melt in the region of the capillary exit. The acceleration subjects the polymer stream to extensional forces with increasing extension rate, reaching around 1 to $3s^{-1}$. The large extensional flow causes slip at the wall of the capillary. The situation may be aggravated by large stresses at the entry to the capillary. As discussed above, the entry stresses are smaller in conical entries, particularly with small cone angles. This point agrees with the quite generally

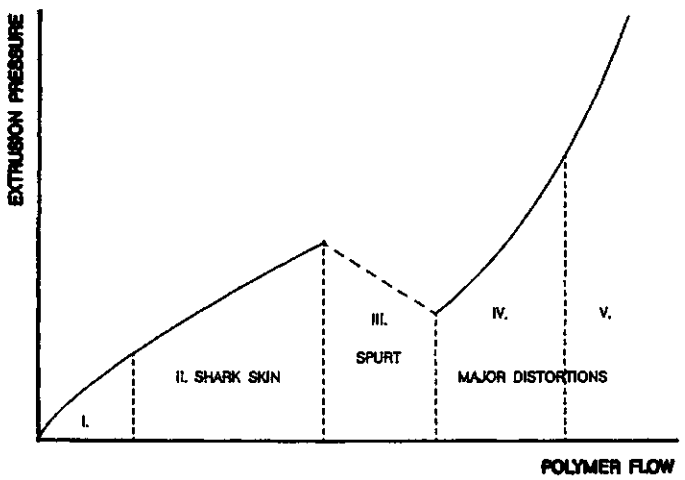

Figure III.16: *A general representation of the relationship between extrusion pressure and flow rate in a capillary extrusion. Section I - extrudate with smooth surface. Section II - extrudate with surface distortions ("shark skin"). Section III - unsteady (oscillatory) or surt flow. Section IV and V - extrudate with major distortions. After Molenaar and Koopman*[58]

known experience (see figure III.16). However, long standing common knowledge is that the geometry of the capillary entrance affects the instabilities (see figure III.17), and in the entry region, the polymer is subjected to extensional forces. Here Hatzikiriakos and Dealy's theory agrees with the facts, however the suggested formalization does not reflect it.

Hatzikiriakos and Dealy[56] have developed a model which describes the fracture phenomena, as represented in figure III.16, quite well. The model has been developed under the following assumptions:

- Viscosity is independent of pressure.
- In the low flow branches, the flow is isothermal.
- Elasticity of the fluid is not taken into account.
- Lubrication approximation is used as creeping flow is assumed.
- For the high flow branch, flat velocity profile (plug flow) is assumed.
- Empirical slip models are used, so slip velocity is taken as being dependant on actual stress (the stress history is neglected).
- Flow above the capillary entry is neglected.
- Normal stresses are calculated from empirical relationships.

The authors[57] conclude that the two most important factors contributing to the melt fracture are compressibility of the melt and slip on the capillary walls.

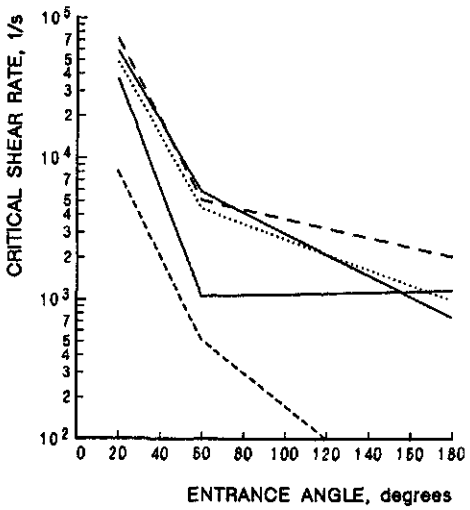

Figure III.17: *Onset of capillary flow instability (critical shear rate) in relation to the angle of capillary entrance cone.*[12]

The authors also suggest that melt elasticity, if accounted for, might improve the agreement between the calculated and experimental results.

Molenaar and Koopmans[58] base their model on the mechanism of relaxation oscillation, according to the earlier suggestion by Weill.[59] To describe the fracture phenomenon , the authors arrive at two coupled differential equations with one parameter:

$$\frac{dQ^*}{dt^*} = \frac{P^* - F^*(\Delta Q^*)}{\varepsilon} \tag{III.198}$$

$$\frac{dP^*}{dt^*} = -\Delta Q^* \tag{III.199}$$

where

$$\varepsilon \equiv \frac{K\, Q_i^2}{C\, P_0^2} \tag{III.200}$$

is a parameter. The notation here is P_0 means a characteristic pressure (taken as equal to $10^7\ Pa$), t is time, t^* is dimensionless time given by

$$t^* \equiv \left(\frac{C\, P_0}{Q_i}\right)^{-1} \cdot t \tag{III.201}$$

$$C \equiv A\, \chi\, h \tag{III.202}$$

A is cross sectional area of the barrel, h is the hight between the plunger and the capillary entry, χ is melt compressibility, Q_i is the inlet flow rate (constant), $Q_e(t)$ is extrudate flow rate. The flow rates are scaled with Q_i so that in the dimensionless form one has

$$Q_e^*(t) \equiv \frac{Q_e(t)}{Q_i} \tag{III.203}$$

and

$$\Delta Q^*(t^*) \equiv \frac{\Delta Q(t)}{Q_i} \tag{III.204}$$

while

$$\Delta Q \equiv Q_e(t) - Q_i \tag{III.205}$$

Naturally, $Q_i \equiv 1$. $P(t)$ is pressure in the barrel as a function of time. In its dimensionless form it is

$$P^*(t^*) \equiv \frac{P(t)}{P_0} \tag{III.206}$$

F is the characteristic material function which may be taken from a constitutive equation of the polymer and of the appropriate boundary conditions. One may write the following relationship between the change of pressure with time to the change of the total mass in the barrel:

$$P(t) = F[\Delta Q(t)] = \int_0^t \frac{Q_i - Q_e(t')}{C(t')}\, dt' \tag{III.207}$$

where $\Delta Q \equiv Q_e(t) - Q_i$.

Further, one may write

$$\frac{d\,[Q_e(t) - Q_i]}{dt} = \frac{d\,Q_e}{dt}\frac{[P - F(\Delta Q)]}{K} \tag{III.208}$$

The dimensionless material function is then

$$F^*(\Delta Q^*) \equiv \frac{[F(\Delta Q)]}{P_0} \tag{III.209}$$

Equation III.198 has only one parameter

$$\varepsilon \equiv \frac{K\,Q_i^2}{C\,P_0^2} \tag{III.210}$$

As results from the above considerations, the onset of "shark skin" (region II in figure III.16) depends only on the constitutive equation. The spurting portion of the curve (region III) is described by self excited oscillation of relaxation of a material which is able to dissipate energy, though energized in a constant way. The shape of the curve depicting the pressure function, $Q_e(t)$, depends on the material properties described by the function F^*. Therefore the behavior in region III depends on the elasticity. Similarly as in region II, in region IV two different stress values correspond to every shear rate. The high shear rate is in the center, the low shear rate, at the wall. This may result in a relatively smooth surface, but major distortions of the extrudate are also likely. The nature of the distortions may depend on a large number of factors related to the material and to the geometry of the hardware.

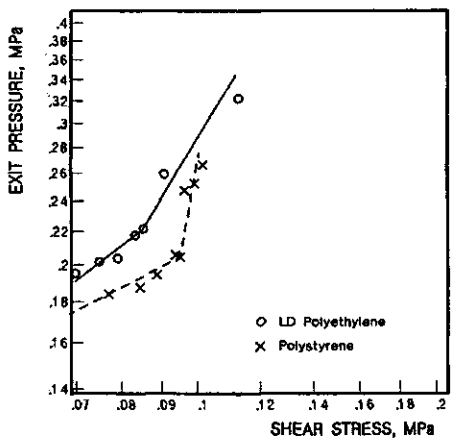

Figure III.18: *Exit pressure in relationship to shear stress. The transition point coincides with the onset of flow instability. After Han and Lamonte.*[62]

It has been noticed that if the angle of the capillary entrance cone is small (figure III.17 and III.18),[12,24] the flow instability starts at higher shear rates (critical shear rate, $\dot{\gamma}_{cr}$). This is consistent with equation III.179. The solution suggested by Molenaar and Koopman[59], in its principle, seems to be more suited to explain the effect of entry geometry. The formalization of the geometric factor still needs additional investigations.

Figure III.18 shows the results of very interesting investigations by Han and Lamonte.[62] The results seem to show convincingly that the elastic properties of a material are quite essential in considerations of flow instabilities.

Vinogradov[63] has determined that flow instabilities appear when stress reaches a critical value, that lies between 0.1 and 0.5 MPa. This value is valid for both shear and extensional deformation, provided that in extension this is the true stress. Vinogradov finds that the value holds for all the polymers known and is little dependent on molecular mass and temperature.

If one translates this to deformation rate, then, obviously, the molecular mass and temperature dependence will appear. The critical stress value is, in physical terms, dictated by the fact that the polymer is unable to accommodate more of reversible deformation. The critical stress value coincides with the exhaustion of the possibilities to further extend the entangled chain segments connecting different molecules. This is equivalent to the inability to accumulate much more of reversible deformation. In effect, at the critical stress, the polymer is forced to a glassy state where it becomes brittle. At this stage, polymers loose adhesion to their boundary surfaces, like capillary walls or plates of rotational rheometers. The last phenomenon causes the spurts from the capillary, the jumpy stress on rotational instruments. In this authors opinion the Vinogradov's suggestion seems to be correct in principle, though the limits for critical behavior appear to vary in a wider range, depending on the viscoelastic character of the polymer and on actual processing conditions.

In the last ten years or so, the attention of researchers has been turned toward the direction which may be termed as the questioning of the notion of zero velocity in a capillary flow. Besides the work quoted above, more evidence of slip on capillary walls has been published. J. Barone and co-workers[69] described a mechanism of local reversible molecular *coil* $\longleftrightarrow$ *stretch* mechanism taking place in the boundary layer at the capillary wall. This mechanism is responsible, on a molecular scale, for an oscillation of stress at the wall and wall slip at the exit of the capillary. This mechanism is considered to be responsible for the formation of *"shark skin"*. The coefficient of friction between the polymer and capillary wall has an influence on the magnitude of the effect. A low friction, *e.g.* achieved through a fluorocarbon coating, at the wall in the exit section of the capillary reduces the shark skin effect. Such a coating also reduces die swell.

M. E. Machay and D. J. Henson[70] found that polystyrene slips at stainless steel walls at all shear rates. The authors were unable to find a theory which would fit the data. They believe that the number of molecules adsorbed at the stainless surface is in a dynamic equilibrium, and this determines the slip behavior.

A. D. Yaring and M. D. Graham[71] have developed a model of the slip at polymer - solid interface. The model shows a fair agreement with published experimental data.

III.8 Molecular Rheology

The abbreviated discussion of rheology given above treats materials as a continuum. This, however, does not exhaust the problem. It is important to realize that ultimately it is the molecular structure of the material that rules over the properties, and certain questions may be answered only through considerations of the molecular structure.

The large size and large length to diameter ratio of polymer chains are the reason for the tendency of molecules to coil into more or less tight bundles. The shape of the coils undergoes constant changes due to natural molecular motions. Therefore, only the average size of the molecule may be calculated or determined (e.g. via light scattering). The molecule size is given usually as the *root mean square end-to-end distance*, $\langle L^2 \rangle^{1/2}$, or as the *root mean square radius of gyration*, $\langle f^2 \rangle^{1/2}$. The two values of unperturbed coils, without any solvent penetration, are related to each other as follows: $\langle L^2 \rangle_0 = 6\langle r^2 \rangle_0$. The average shape of the molecule coil is somewhat elongated, kidney-like, rather than spherical. Increase in chain branching results in the coil shape changing to more spherical. With the increasing rigidity of the chains, the chain dimensions increase, eventually approaching the shape of a rod, e.g. polymers forming liquid crystals.

In the unperturbed state, the radius of gyration of a polymer of given architecture is a function of molecular mass: $\langle r^2 \rangle_0 = KM$. For rod shape molecules, however, the relationship is $\langle r^2 \rangle_0 = KM^2$.

Based on Zimm's theory, the relaxation time of a polymer, θ, may be calculated

from the following relationship:

$$\theta = \frac{M(\eta_0 - \eta_s)}{(2.369\ c\ R\ T)} \tag{III.211}$$

where η_0 is zero-shear viscosity, η_s is viscosity of solvent, c represents solution concentration, and M, R, T have the usual meaning. For undiluted polymers, solvent viscosity becomes zero and polymer concentration is to be substituted with polymer density. The constant of 2.369 has been found by Tschoegl[30] to vary from $\pi^2/6$ to 2.369 as the shielding parameter varies from zero (for vanishing hydrodynamic interaction in the free draining coil) to infinity (for dominant hydrodynamic interaction). Temperature dependence of relaxation time is formulated as

$$\theta = \theta_0\ \frac{T_0\ \eta(T)}{T\ \eta(T_0)} \tag{III.212}$$

where the subscript zero designates the data at the reference temperature of T_0.

For polymers of low molecular mass (oligomers), up to a certain critical value of molecular mass, M_c, zero-shear melt viscosity is directly proportional to weight average molecular mass, M_w. In a double logarithmic plot, this gives a straight line of slope equaling one. Above the critical molecular mass, however, the relationship is

$$eta_0 = KM_w^{3.4} \tag{III.213}$$

How viscosity at non-zero shear rates deviates from equation III.213 may be seen from figure III.19. The shear rate related deviations have not been quantified yet.

The intersections of the line representing low molecular mass polymers (slope one) with the lines for non-zero shear rates indicate the points beyond which the polymer will be degraded due to the shear action. Based on this principle, another graph for polymer degradation may be constructed; an example is given in figure III.20.[31]

Temperature dependence of zero-shear viscosity may be described by the Arrhenius type equation:

$$\eta_0 = A_m \exp(E/R\ T) \tag{III.214}$$

where A_m a constant and E is activation energy of flow. However, both the activation energy and the pre-exponential factor depend on temperature and time, and therefore the equation is not general. Another solution has been proposed by H. Leaderman and furthered by Ferry, Tobolsky, Staverman, Schwartl: the so called shift factor, usually represented by a. The equation represents indeed a time-temperature equivalence shift factor. The shift factor represents a means by which such curves as shear modulus *versus* temperature, or stress relaxation modulus *versus* time and temperature, or viscosity *versus* temperature may be represented by a single *master curve* for each of the dependent variables. The effect of temperature change may be calculated by multiplying all values by a

common factor, $a(T)$, which is a function of temperature and which represents the equivalence of time and temperature.

$$\ln a = f(T) - f(T_0) \tag{III.215}$$

where T_0 is a reference temperature, a target temperature to which one attempts

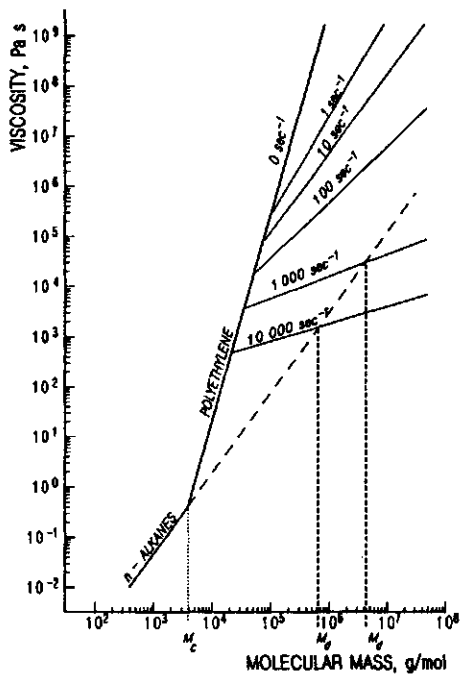

Figure III.19: *Relationship between melt viscosity and molecular mass of polyethylene, parameter: shear rate. M_D is the molecular mass beyond which the polymer will be degraded by respective shear rate. Data after H. P. Schreiber, E. B. Bagley, and D. C. West.*[31]

to recalculate the data.

Interpretation of rheology through chain entanglements[65] gives the following interpretation of the shift factor.

$$a = \ln\left(\frac{\theta}{\theta_g}\right) = \ln\left(\frac{\theta_0}{\theta_{0g}}\right) + 2\ln\left(\frac{E}{E_g}\right) \tag{III.216}$$

where θ is relaxation time, E is modulus of elasticity, the subscripts stand for: 0 related to the unit segment between entanglements, g at glass transition. From this equation one may also derive the WLF equation.[65]

The most frequently used equation for the shift factor is:

$$a = \frac{\rho_0 T_0}{\eta_0}\frac{\eta}{\rho T} \tag{III.217}$$

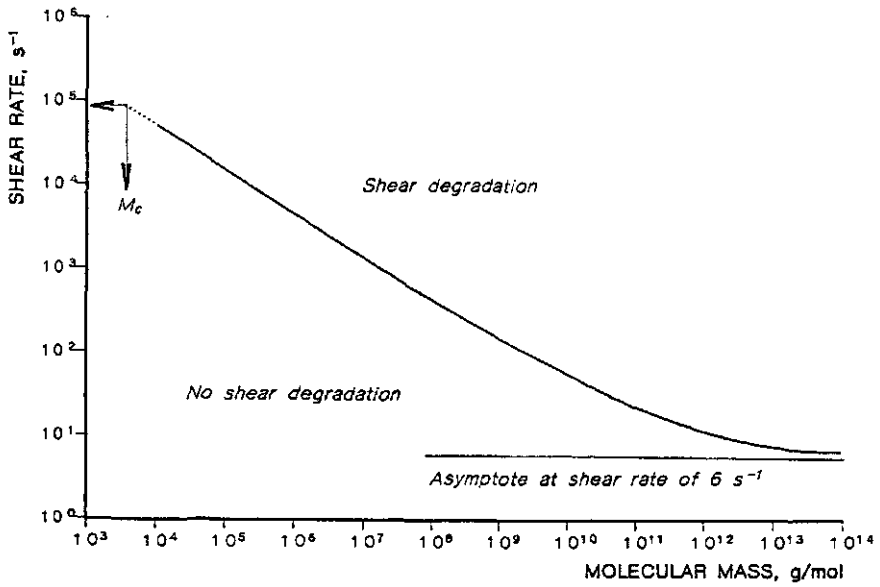

Figure III.20: *Degrading shear rate for polymer of a given molecular mass. Graph constructed on the basis of Figure III.19 for polyethylene.*[31]

where the symbols have their customary meaning, and subscript 0 represents values at the reference temperature. Other equations of frequent use are:

$$\frac{\rho_0 T_0}{\rho T} G(t \cdot a, T) = G(T_0, t) \tag{III.218}$$

$$\frac{\rho_0 T_0}{\rho T} G'(\omega/a, T) = G'(T_0, \omega) \tag{III.218 a}$$

$$\frac{\rho_0 T_0}{\rho T} G''(\omega/a, T) = G''(T_0, \omega) \tag{III.218 b}$$

$$\frac{\rho T}{\rho_0 T_0} J(t \cdot a, T) = J(T_0, t) \tag{III.219}$$

$$\frac{\rho T}{\rho_0 T_0} J'(\omega/a, T) = J'(T_0, \omega) \tag{III.219 a}$$

$$\frac{\rho T}{\rho_0 T_0} J''(\omega/a, T) = J''(T_0, \omega) \tag{III.219 b}$$

In equations III.215 and III.217, the meaning of the symbols is as throughout this chapter.

Considering equation III.215,[63] a simpler, though not so general, way of determining the a-factor has been devised specifically for some polymers. For polypropylene, equation III.220 has been found to be quite satisfactory. It, like other equations of similar type, is based on experimental results. Such equations are

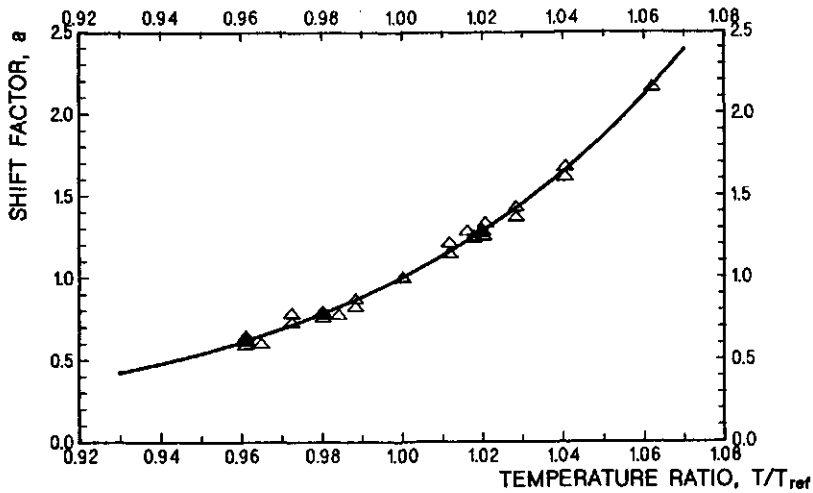

Figure III.21: *Dependence of the shift factor, a, on the ratio of temperatures. The relation has been devised for polypropylene on the basis of experimental data.*

convenient, especially when interpolations or extrapolations are needed. The extrapolated data are particularly convenient for considerations of crystallization, since rheological determinations below equilibrium melting point are rarely reliable, or even possible.

$$a = 4.129 \cdot 10^{-6} \cdot \exp\left[12,4260\left(\frac{T}{T_0}\right)\right] \tag{III.220}$$

Figure III.21 presents the original data for various propylene polymers and their agreement with equation III.220.

Williams, Landell, and Ferry have developed an equation, usually called the *WLF equation*[32], to calculate activation energy. This equation has been developed on the basis of considerations of the segmental motions in molecules. One of the many forms of the equation is

$$\log \eta(T) = \log \eta(T_s) - \frac{8.86\ (T - T_s)}{101.6 + (T - T_s)} \tag{III.221}$$

where the reference temperature is $T_s = T_g + 43$. For the majority of crystallizing polymers, this equation is inapplicable as at forty three degrees above glass transition the polymers are solids. Another form of the WLF equation that may be used is:

$$E(T) = \frac{4120\ T}{(51.6 + T - Tg)} \tag{III.222}$$

The activation energy so calculated is of acceptable accuracy for a temperature that is by no means higher than fifty degrees above glass transition, and preferably by no more than twenty degrees above glass transition. The activation energy so calculated may be used in equation III.214. An empirically determined activation energy of flow gives a straight line which has one point in common with the WLF

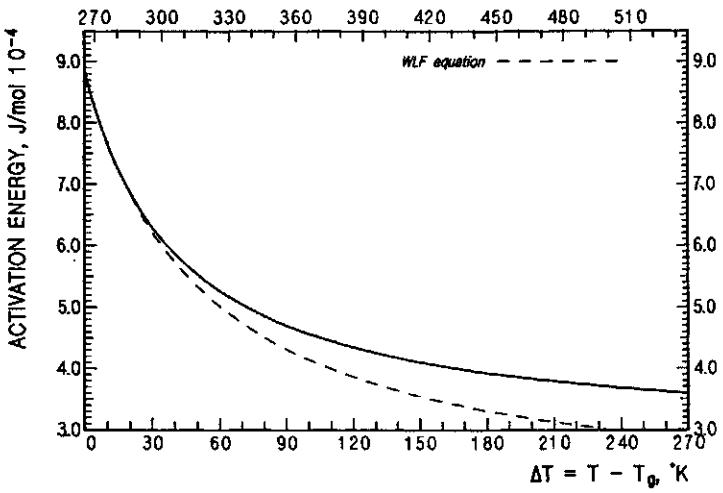

Figure III.22: *Activation energy of flow as calculated from WLF equation (dashed line) as compared to the activation energy calculated using equation III.223.*

hyperbolic equation: it is the point at glass transition temperature. The new equation has been found to hold well for polypropylene over the entire range of temperature, though its validity for other polymers needs to be established.[33] Possibly, the equation coefficients may be different for other polymers. The difference between the original WLF equation and the proposed modification may be seen in Figure III.22.

$$E(T) = T_g \ [334.29488 - 0.56625 \ (T - Tg)] \tag{III.223}$$

The equation yields the energy in J/mol. The activation energy may be used either with Arrhenius equation (III.214) or with another empirical equation, III.224 - III.225, relating both temperature and shear rate. Again, equation III.224 - III.225 has been corroborated with the experimental data on polypropylenes of a wide range of molecular masses; its validity for other polymers remains to be determined. .

$$\eta_0 = A_m \ \exp\left(\frac{E \ A_{\dot{\gamma}}}{R \ T}\right) \tag{III.224}$$

where

$$A_{\dot{\gamma}} = \frac{1 + l \ \dot{\gamma}^{1/2}}{1 + m \ \dot{\gamma}^{1/2}} \tag{III.225}$$

Here l and m are empirical constants which may be calculated by fitting experimental data into equations III.214 and III.223; correlation coefficients on the order of 0.999 or even 0.9999 are obtainable over six or eight decades of shear rates.[33] The coefficients in equation III.223 have no general validity, since every polymer batch needs a separate determination. Nevertheless, these kinds of empirical correlations serve as exceptionally convenient algorithms for various interpolations, *e. g.* such as are often needed in computerized data evaluation or predictions where

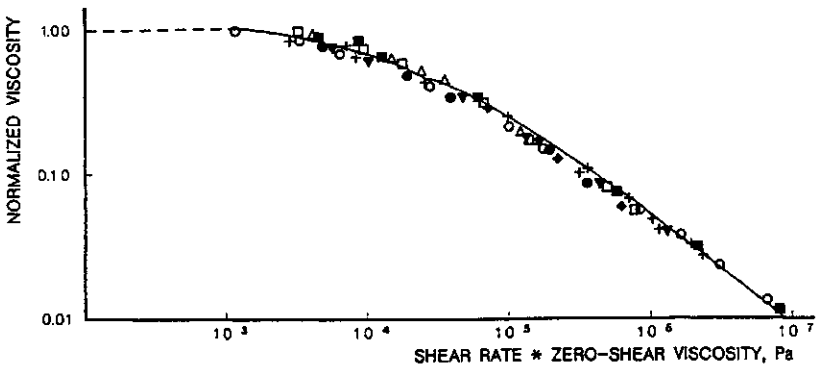

Figure III.23: *Relationship between reduced viscosity and product of shear rate and zero-shear rate viscosity, a temperature independent function. After Vinogradov and Mal'kin.*[34]

the points must be generated very densely. On many occasions, the solutions backed by full theoretical justification are not broad enough to serve the purpose.

Still another way of relating viscosity and temperature and shear rate is suggested by Vinogradov and Mal'kin,[34] who find that the reduced viscosity (ratio of viscosity at any shear rate over zero-shear rate viscosity) is a temperature independent function of the product of zero-shear rate viscosity and shear rate, $(\eta_0\dot{\gamma})$ as indicated in figure III.23.[34]

The solution suggested by Vinogradov and Mal'kin must be treated as an empirical one, similarly to other proposals which lack sufficient theoretical backing.

III.9 Viscosity of Solutions

Staudinger derived the following equations to describe the relationship between molecular mass of a polymer, solvent viscosity, and solution concentration, on one side, and viscosity of solution, on the other side:

$$[\eta] = K_m\ M \tag{III.226}$$

where $[\eta]$ is intrinsic viscosity defined as

$$\lim_{c\to 0} \frac{\eta - \eta_s}{c_s} = [\eta] \tag{III.227}$$

η is viscosity of polymer solution at concentration c, s is the viscosity of pure solvent, K_m represents a polymer characteristic constant, and M stands for the molecular mass. Staudinger's equation has been modified to improve its agreement in confrontation with experiment. In its present form, often called the Mark-Houwink equation, it has the following form:[35,36]

$$[\eta] = K\ M^{\alpha} \tag{III.228}$$

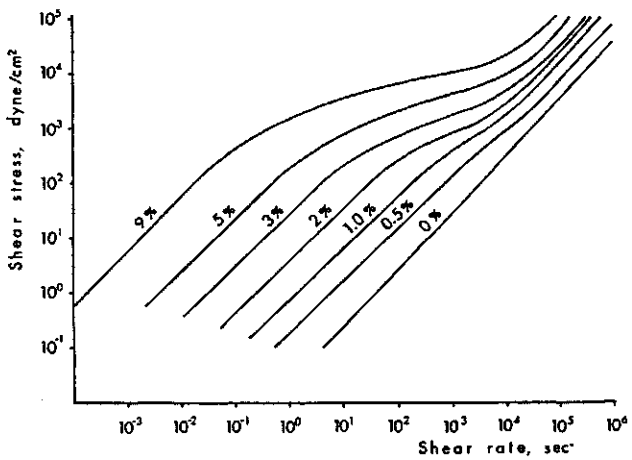

Figure III.24: *Shear stress as a function of shear rate for low to moderate concentrations of polyisobutylene in decalin.*[38]

Here α is a constant assuming values between 0.5 and 1.0, depending on solvent - polymer interaction. A value of $\alpha = 0.5$ corresponds to a system very close to precipitation (so called *theta solvent*, and $\alpha = 1$ means very good solubility. Extensive tabulations of the values of K and α may be found in literature.[37]

The Mark-Houwink equation is valid for diluted solutions only, where there is practically no interaction between the solute molecules. If one considers moderately or highly concentrated solutions as continuum systems, then all that has been said on rheology applies also to solutions. The difference may be that the general level of stresses is probably lower. In molecular terms, however, there are somewhat different problems involved. Unfortunately, the problems have not been fully solved yet. On the other hand, since polymer concentrations used in fiber formation range from under ten per cent to some sixty per cent, the behavior of concentrated solutions is technologically more interesting.

Brodnyan, Gaskins and Philipoff[38] have studied solutions of polyisobutylene in decalin. The quintessence of this work is presented in figure III.24. Qualitatively similar results have been obtained for other polymer solvent systems. As it is evident from figure III.24, the shape of the shear stress-shear rate function changes with concentration. In order to predict viscosities of concentrated polymer solutions, one may use equation III.211. However, knowledge of the relaxation time would be required, and usually this is not readily on hand. The attempts, which have been crowned with some success, to explain these variabilities have been based on the theory of free volume.

Free volume may be loosely described as the empty space between molecules resulting from the irregular structure of the molecules filling a volume, or shortly, a molecule packing effect.[39] The internal friction in liquids is related to the free volume, v_f.[40] Doolittle,[41] based on empirical grounds, has proposed the following

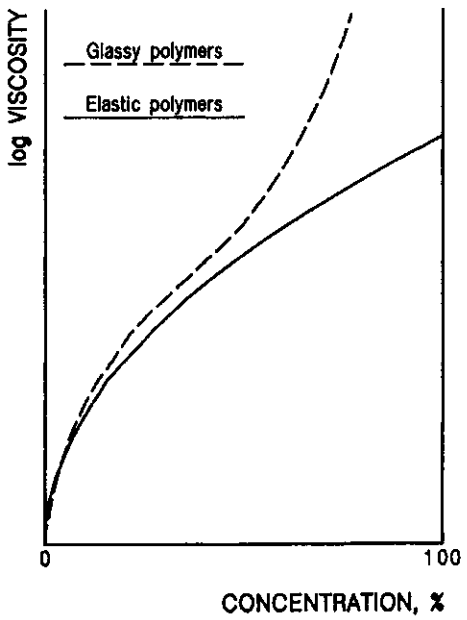

Figure III.25: *Generalized dependence of solution viscosity on the concentration of elastic and glassy polymers.*[39]

description of the relationship between free volume and viscosity:

$$\eta = A \ \exp(B \ v_0/v_f) \tag{III.229}$$

Here η is viscosity of solution, v_0 is the occupied volume, v_f is free volume, A and B are coefficients. The general dependence of solution viscosity on concentration has been given in graphic form by Tager and Dreval.[39] This curve is presented in figure III.25. It is worth stressing the relatively small increase of viscosity with increasing concentration once somewhat higher concentration levels are reached. For elastic polymers the slope is particularly low.

It is believed that solvents have larger free volume. Also, free volume is believed to be an additive property. Fujita and Kishimoto[42] assume the free volume of a solution to increase with increasing volume of solvent. Free volume depends also on the polymer concentration and on temperature of solution. Based on such considerations, these authors derived the following equation.

$$-\frac{1}{\ln a_c} = f(T\phi_*) + \frac{f(T\phi^*)}{\beta'(T)} \times \frac{1}{\phi - \phi^*} \tag{III.230}$$

in which

$$a_c = \frac{\eta(T\phi)(1-\phi^*)}{\eta(T\phi^*)(1-\phi)} \tag{III.230 a}$$

where $\eta(T\phi)$ is viscosity at temperature T and volume fraction of solvent ϕ, $\eta(T\phi*)$ is viscosity at the same temperature and another volume fraction of solvent ϕ^*,

considered as a comparative standard, $f(T\phi^*)$ is free volume of solution at standard concentration, $\beta'(T) = \gamma(T) - f(T_0), \gamma(T)$ is a function specific for given polymer-solvent system, and $f(T_0)$ is free volume of solvent at temperature T_0.

Equation III.230 may be simplified to a rectilinear form so the values of $\beta'(T)$ and $f(T\phi^*)$ may be obtained more easily:

$$-\frac{1}{\ln a_c} = F\,\frac{1}{(1-\phi^*)} \qquad (III.230\,b)$$

Validity of equation III.230b has been confirmed for many polymer-solvent systems. The rectilinearity appears to falter at ϕ larger than 0.5.[39,42–45]

Another approach to the problem has been offered by Kelly and Bueche,[46] who assume the free volume of a polymer to be

$$v_{fp} = 0.025 + 4.8 \cdot 10^{-4}(T - T_g) \qquad (III.231)$$

and the free volume of solvent as

$$v_{fs} = 0.025 + \alpha_S(T - T_{gs}) \qquad (III.232)$$

The notation here is: v_{fp} stands for free volume of polymer, v_{fs} stands for free volume of solvent, the coefficient of 0.025 represents the relative free volume of the polymer at glass transition, the value of $4.8 \cdot 10^{-4}(^oK)^{-1}$ is the temperature coefficient of changes of the free volume, S is a temperature coefficient of the order of $10^{-3}(^oK)^{-1}$. Further, under the assumption of the additivity of free volumes, Kelly and Bueche obtain

$$\begin{aligned}\frac{\ln\eta}{B} = \;& 4\,\ln\rho\,\{\phi_p\,[0.025 + 4.8\cdot 10^{-4}(T - T_g)] + \\ + \;& (1-\phi_p)\,[0.025 + \alpha_S(T - T_{gs})]\}^{-1}\end{aligned} \qquad (III.233)$$

where ρ is density of the solution, ϕ_s and ϕ_p volume fractions of solvent and polymer, respectively, and B is a parameter which also includes molecular mass. Equation III.233 is in good agreement with experiment at temperatures above glass transition temperature of the polymer.

Several other equations for the dependence of viscosity on solution concentration may be found in the literature.[47,48]

Molecular mass has an influence on the solution viscosity similar to that on the melt viscosity. An equation entirely analogous to that for melts (equation III.213) may be written as

$$\eta = C\,P^{3.4} = K\,c^m\,M^{3.4} \qquad (III.234)$$

where P is degree of polymerization, and C and K are constants, c is the solution concentration. The exponent m varies between 4 and 5.6; the higher values are more likely to be valid at higher concentrations. For polymer below the

critical molecular mass, the slope is not constant and increases with increasing concentration.[39,49]

The influence of molecular mass on viscosity may also be obtained from equation III.211.

Another important function is the viscosity as a function of temperature. The activation energy of flow has a nonlinear dependence on concentration[39] and on molecular mass.[49–53] Consequently, the WLF equation is inapplicable here. Teramoto, Okada, and Fujita[49] have proposed a somewhat different relationship:

$$\frac{T - T_0}{\lg a_T} = \frac{[f(\phi T_0)]^2}{a_f(\phi)} + (T - T_0)\, f(\phi\, T_0) \qquad \text{(III.235)}$$

$$a_T = \frac{\eta(\phi\, T)}{\eta(\phi\, T_0)} \qquad (III.235\,a)$$

where T and T_0 are experiment and reference temperature, respectively, $f(\phi T_0)$ is free volume of solution at polymer volume fraction ϕ and at reference temperature T_0. The equation may be easily linearized by substituting $(T - T_0)/\lg a_T = f(T)$, and in this way all of the important parameters may be estimated.

There have been many different attempts to solve the relationship between viscosity, solution concentration, temperature, and molecular mass. Some of the theories agree with experiment only within limited ranges. The selection given here does not imply any particular preference.

The character of the solvent used has an influence on the solution viscosity. This influence becomes even stronger below the glass transition temperature of the polymer. The solvent quality also influences how strongly temperature influences viscosity. Also, the quality of solvent influences the activation energy of solution flow.[39] Viscosities of solutions do not necessarily depend on the viscosities of the solvents used. This is related to the changes of entropy upon dissolution. Viscosity is lower in those solvents which permit more flexibility of polymer chains. Naturally, the solvent viscosity will superimpose itself on the effect.

In concentrated polymer solutions, molecular interactions are appropriately high. Longer times are needed to reach thermodynamic equilibrium. The significance of these phenomena increases with increasing polarity of the polymer molecules. Increase of viscosity with time is one of the common properties of the concentrated solutions. It is usually called *aging* or *ripening* of the solution. The rate of such a process depends both on temperature and on agitation, and on the whole thermal and shear history of the solution. In this case, the concentration of polymer solutions is also important, the rate of viscosity increases is magnified by increasing concentration.[55,56] Different polymer-solvent systems may behave quite differently. This makes it exceedingly difficult to determine the exact mechanisms involved in the processes of solution aging. Since the viscosity of solutions increases on aging, it may be generally assumed that some kind of molecular association takes place. Depending on the type of association, molecular entanglements, molecular mobility, the rate of equilibration varies widely. There

are no quantitative theories related to this problem, every polymer-solvent system must be studied separately.

III.10 References

1. N. W. Tschoegl: *Phenomenological Theory of Linear Viscoeastic Behavior*, Springer Verlag, Berlin-Heidelberg-New York, 1989.
2. J. D. Ferry: *Viscoelestic Properties of Polymers*, John Wiley & Sons Publ., New York, 1980.
3. I. Emri, N. W. Tschoegl, *Rheol. Acta*, **32 (1993)**, 311, 327.
4. N. W. Tschoegl, *Seminar for Kimberly-Clark Corp.*, Roswell, Ga., Sept. 24, 1993.
5. V. M. Kamath, M. R. Mackley, *J. Non-Newtonian. Fluid Mech.*, **32 (1989)**, 119.
6. M. Baumgartel, H. H. Winter, *Rheol. Acta*, **28 (1989)**, 511.
7. V. Capuccio, A. Coen, F. Bertinotti, and W. Conti, *Chim. e Ind. (Milano)*, **44 (1962)**, 463.
8. E. B. Bagley, S. H. Storey, and D. C. West, *J. Appl. Polymer Sci.*, **7 (1963)**, 1661.
9. W. Philipoff and F. H. Gaskins, *Trans. Soc. Rheology*, **2, (1958)**, 263.
10. F. N. Cogswell, *Rheol. Acta*, **8 (1969)**, 187.
11. F. N. Cogswell, *Polymer Eng. Sci.*, **12 (1972)**, 64.
12. Z. K. Walczak: *Formation of Synthetic Fibers*, Gordon and Breach, London - New York, 1977, Chapter 2.
13. H. P. Hurlimann and W. Knappe, *Rheol. Acta*, **11 (1972)**, 292.
14. A. B. Metzner and A. P. Metzner, *Rheol. Acta*, **9 (1970)**, 174; **10 (1971)**, 434.
15. M. Zidan, *Rheol. Acta*, **8 (1969)**, 89.
16. S. L. Goren, *J. Fluid Mech.*, **25 (1966)**, 87.
17. S. L. Goren and S. Wronski, *J. Fluid Mech.*, **25 (1966)**, 185.
18. J. Gavis and M. Madon, *Phys. Fluids*, **10 (1967)**, 487. 18
19. J. L. White, *J. Appl, Polymer Sci.*, **8 (1964)**, 2339. 19
20. P. Lamb, *S.C.I. Monograph*, **26 (1967)**,296.
21. J. Vlachopoulos and M. Alam, *Polymer Eng. Sci.*, **12 (1972)**, 184.
22. E. B. Bagley, *Trans. Soc. Rheology*, **5 (1961)**, 355.
23. R. S. Spenser and R. E. Dillon, *J. Colloid Sci.*, **4 (1949)**, 251.
24. J. F. Tordella, *J. Appl. Phys.*, **27 (1956)**, 454.
25. R. T. Balmer and J. J. Kauzlarich, *A. I. Ch. E., J.*, **12, (1971)**, 1181.
26. J. R. A. Pearson, *Trans., J. Plast. Inst.*, **37 (1969)**, 285.
27. R. T. Balmer, *J. Appl. Polymer Sci.*, **18 (1974)**, 3127. 27
28. F. W. Cogswell, *Trans. Soc. Rheol.*, **16 (1972)**, 383. 28

29. B. H. Bersted, *Polymer Eng. Sci.*, **33 (1993)**, 1079.

30. N. W. Tschoegl, *J. Chem. Phys.*, **39 (1963)**, 149; **40 (1964)**, 473.

31. H. P. Schreiber, E. B. Bagley, and D. C. West, *Polymer*, **4, (1963)**, 355.

32. M. L. Williams, R. F. Landel, and J. D. Ferry, *J. Am. Chem. Soc.*, **77 (1955)**, 3701.

33. Z. K. Walczak, *previously unpublished results*, 1986.

34. G. V. Vinogradov, A. Ya. Mal'kin: *Reologiya polimerov (Rheology of polymers)*, Izdatelstvo Chimija, Moskva, 1977, p. 227-228; *Rheology of Polymers*, Springer Verlag, Berlin -Heidelberg - New York, 1980.

35. W. Kuhn, *Kolloid-Z.*, **62 (1933)**, 269; **68 (1934)**, 2.

36. R. Houwink, *J. prakt. Chem.*, **157 (1940)**, 15.

37. J. Brandrup and E. H. Immergut (Eds.), *Polymer Handbook*, Interscience Publ., New York, 1966, Chapter 4.

38. J. D. Brodnyan, F. H. Gaskins, and W. Philipoff, *Trans. Soc. Rheol.*, **1 (1957)**, 109.

39. A. A. Tager and V. E. Dreval, *Uspyekhy Khim.*, **36,(1967)**, 888.

40. A. I. Batschinskij, *Z. physik. Chem.*, **84 (1913)**, 6 , 143.

41. A. K. Doolittle, *J. Appl. Phys.*, **22 (1951)**, 1471; **23 (1952)**, 236.

42. H. Fujita and A. Kishimoto, *J. Chem. Phys.*, **34 (1961)**, 393.

43. J. Ferry, L. D. Grandine, Jr., and D. C. Udy, *J. Colloid Sci.*, **8 (1953)**, 529.

44. F. Bueche, *J. Appl. Phys.*, **24 (1953)**, 423; **30 (1959)**, 1114.

45. H. Fujita and E. Maekawa, *J. Phys. Chem.*, **66 (1962)**, 1053.

46. F. N. Kelly and F. Bueche, *J. Polymer Sci.*, **50 (1961)**, 549.

47. L. J. Zapas, *ACS, Polymer Preprints*, **15(No. 2)(1974)**, 131.

48. J. W. Van Krevelen: *Properties of Polymers*, Elsevier Publ., Amsterdam - London - New York, 1990, Chapter 19.

49. A. A. Tager, V. E. Dreval, and N. G. Trayanova, *Dokl. Akad. Nauk USSR*, **151 (1963)**, 140.

50. J. Oyanagi and M. Matsumoto, *J. Colloid Sci.*, **17 (1962)**, 426.

51. S. Yugushi, *Chem. High. Polymers (Japan)*, **19 (1962)**, 113.

52. R. F. Landel, J. W. Berge, and J. D. Ferry, *J. Colloid Sci.*, **12 (1957)**, 400.

53. R. S. Porter and J. F. Johnson, *J. Polymer Sci.*, **3 (1962)**, 11.

54. A. Teramoto, R. Okada, and H. Fujita, *J. Phys. Chem.*, **66, (1962)**, 1228.

55. S. Zahorski, *Arch. Mech.*, **23 (1971)**, 1433; **24 (1972)**, 681.

56. S. G. Hatzikiriakos and J. M. Dealy, *J. Rheol.*, **36 (1992)**, 845.

57. S. G. Hatzikiriakos, *Polymer Eng. Sci.*, **34 (1994)**, 1441.

58. J. Molenaar and R. J. Koopmans, *J. Rheol.*, **38 (1994)**, 99.

59. A. Weill, *Rheol. Acta*, **19 (1980)**, 623.

60. F. Sugeng, N. Phan - Thien, R. I. Tanner, *J. Rheology*, **31 (1987)**, 37.

61. C. R. Beverly, R. I. Tanner, *J. Rheology*, **33 (1989)**, 989.

62. C. D. Han and R.R. Lamonte, *Polymer Eng. Sci.*, **11 (1971)**, 385.

63. V. A. Vinogradov, *Rheol. Acta*, **14 (1975)**, 942.

64. A. J. Staverman and F. Schwartzl: *Linear Deformation Behaviour of High Polymers* in *Die Physik der Hochpolymeren*, Ed. H. A. Stuart, Springer Verlag, 1954, Vol. 4, p 56 ff.

65. J. Furukawa, *J. Appl. Polymer Sci.*, **57 (1995)**, 1085; 1095.

66. A. V. Pendse and J. R. Collier, *J. Appl. Polymer Sci.*, **59 (1996)**, 1305.

67. J. R. Collier, O. Romanoschi, and S. Petrovan, *J. Appl. Polymer Sci.*, **69 (1998)**, 2357.

68. N. W. Tschoegl, *Kolloid-Z.*, **174 (1961)**, 113.

69. J. R. Barone, N. Plucktavaesak, and S. Q. Wang, *J. Rheol.*, **42 (1998)**, 813.

70. M. E. Mackay and D. J. Henson, *J. Rhoel.*, **42 (1998)**, 1505.

71. A. L. Yarin and M. D. Graham, *J. Rheol.*, **42 (1998)**, 1491.

72. Y. Termonia, *J. Polymer Sci., Pt. B, Polymer Phys.*, **38 (2000)**, 2422.